# ROLE OF ALTERNATIVE SPLICING FACTOR MBNL1 IN PATHOGENESIS OF MYOTONIC DYSTROPHY

By

JIHAE SHIN

A DISSERTATION PRESENTED TO THE GRADUATE SCHOOL
OF THE UNIVERSITY OF FLORIDA IN PARTIAL FULFILLMENT
OF THE REQUIREMENTS FOR THE DEGREE OF
DOCTOR OF PHILOSOPHY

UNIVERSITY OF FLORIDA

2009

To my parents

ACKNOWLEDGEMENTS

First and foremost, I would like to thank my mentor Dr. Maurice Swanson. I have been amazingly fortunate to have an advisor who is extremely patient, supportive and thinks the best of his students. He was always available to discuss research projects as well as other issues important to my career as a scientist. Once he told me that most students imprint on their mentors. I just hope I have effectively imprinted during my thesis work since he is an exceptional scientist with persistence, passion, curiosity and creativity.

I would like to thank my committee members, Drs. Brian Harfe, Hideko Kasahara and Paul Oh for their direction, dedication and invaluable suggestions during my graduate study. I am grateful to Dr. Laura Ranum at University of Minnesota for her encouragement and support for my career. I thank my colleagues in the Swanson lab who all became great friends, especially Yuan Yuan, Michael Poulos, Jason O'Rourke, Konstantinos Charizanis and Ranjan Batra. Their friendship made my years in graduate school very enjoyable and their passion and enthusiasm for research was truly inspirational. I also acknowledge Joyce Connors for her outstanding support in handling administration.

This dissertation would not have been possible without the invaluable help and contributions of many people. I would like to thank former lab members Drs. Rahul Kanadia and Dan Tuttle as well as my collaborators Drs. Stuart Beattie, Thurman Wheeler, Charles Thornton, Jennifer Embury, Changquing Xia and Glenn Walter. The technical support of Fan Ye was also essential for this study.

I am also indebted to my wonderful advisors during my undergraduate studies. Dr. Kunsoo Rhee at Seoul National University and Dr. Ryoichi Matsuda at the University of Tokyo gave me priceless advice and guidance when I was most uncertain about my future and career.

Last but not least, I would like to thank my family. I am grateful to my parents, Bokyeong Heo and Bukyun Shin for their unconditional love and support. They have always had faith and confidence in me, which has been my source of strength for these years. I also thank my loving brother and sister, Hyunseung and Jiyeon Shin who have been my best friends. I would like to thank my little dog Hiro Shin for making me smile and still feel at home when I am thousands of miles away.

TABLE OF CONTENTS

page

LIST OF TABLES

LIST OF FIGURES

LIST OF ABBEREVIATIONS

| | |
|---|---|
| DM | myotonic dystrophy |
| UTR | untranslated region |
| ds RNA | double stranded RNA |
| HSA | human skeletal actin |
| MBNL | muscleblind-like |
| CELF | CUGBP1/ETR-3-like factors |
| Tnnt | troponin T |
| Clcn | chloride channel |
| NMD | nonsense mediated decay |
| AON | antisense oligonucleotide |
| AAV | adeno-associated virus |
| CF | cystic fibrosis |
| P | postnatal day |
| TA | tibialis anterior |
| SR | sarcoplasmic reticulum |
| Ryr | ryanodine receptor |
| Serca | SR/endoplasmic reticulum $Ca^{2+}$ ATPase |
| Ca | calcium |
| f | fetal |
| H&E | hematoxylin and eosin |
| Bl6 | C57BL/6 |
| 129 | 129/Sv |
| T1/2R | time to half relaxation |
| NMJ | neuromuscular junction |

| | |
|---|---|
| AChR | acetylcholine receptor |
| nt | nucleotide |
| KO | knockout |

Abstract of Dissertation Presented to the Graduate School
of the University of Florida in Partial Fulfillment of the
Requirements for the Degree of Doctor of Philosophy

# ROLE OF ALTERNATIVE SPLICING FACTOR MBNL1 IN PATHOGENESIS OF MYOTONIC DYSTROPHY

By

Jihae Shin

December 2009

Chair: Maurice Swanson
Major: Medical Sciences—Genetics

Myotonic dystrophy (DM) is an RNA-mediated disease caused by a non-coding CTG repeat expansion in the DMPK gene (DM type 1, DM1) or a CCTG expansion in ZNF9 (DM type 2, DM2). Pathogenesis of DM involves dysregulation of alternative splicing factors such as the MBNL1 protein. MBNL1 is sequestered by mutant transcripts containing C(C)UG repeat RNAs which form discrete nuclear RNA foci that, in turn, leads to the loss of MBNL1 function. Because MBNL1 is an RNA binding protein that regulates alternative splicing of a specific subset of pre-mRNAs during postnatal development, loss of this splicing factor due to its sequestration results in missplicing of MBNL1 target pre-mRNAs and perturbation of developmental signals. DM is a systemic disease that affects multiple organs and key features of this disease include myotonia (hyperexcitability of muscle), myopathy (muscle weakness), cardiac conduction defects and subcapsular cataracts. However DM1 is also remarkably variable in severity and penetrance mainly due to somatic mosaicism of CTG repeat size but also due to the variability in genetic background between individuals. We hypothesized that MBNL1 loss of function due to

sequestration is a primary pathogenic event in DM and is responsible for disease-associated phenotypes owing to the failure of developmental transitions as a result of mistakes in alternative splicing. In this study, we show that overexpression of Mbnl1 in vivo mediated by transduction of skeletal muscle with a recombinant adeno-associated viral vector is sufficient to rescue myotonia and missplicing in the *HSA*$^{LR}$ poly(CUG) mouse model for DM, suggesting that loss of MBNL1 activity is primarily responsible for disease pathogenesis. We also report that Mbnl1 deficiency leads to defects not only in skeletal muscle but also other organs like thymus and skin in *Mbnl1* knockout mice depending on the genetic background. This observation indicates that MBNL1 has a broad role in developmental pathways. Furthermore, using congenic *Mbnl1* knockout mice, we provide evidence that functional and structural muscle abnormalities in DM may be separable from myotonia and may be attributed to the altered splicing of genes important for calcium homeostasis, including the ryanodine receptor. Our results suggest a fundamental role of MBNL1 in development and disease and provide a theoretical and experimental basis for the development of novel therapies for this neuromuscular disease.

# CHAPTER 1
# GENETIC COMPLEMENTATION OF MBNL1 REVERSES MYOTONIA AND MISSPLICING IN A POLY(CUG) MOUSE MODEL FOR MYOTONIC DYSTROPHY

## Introduction

### Alternative Splicing during Post-natal Development

During mammalian postnatal development, many organs undergo dramatic morphological changes, which require precise regulation of gene expression. For example, during embryonic myogenesis, myoblasts of somatic origin proliferate and fuse to form multinucleated myofibers, which require high expression of myogenic proteins. On the other hand, postnatal growth of skeletal muscle is achieved by hypertrophy rather than an increase in fiber numbers and this process demands high levels of contractile proteins. Regulation of gene expression during this developmental transition is controlled in a complex, yet very coordinated, manner with the involvement of multiple layers of regulatory machinery including transcription, mRNA processing as well as translation.

Alternative splicing is a critical step for the expression of most genes in eukaryotic cells and it is a very efficient way to generate a variety of proteins that are physiologically and functionally distinct from the limited gene pool. For many tissues including skeletal muscle, expression of subsets of developmentally regulated genes is controlled by temporal and spatial regulation of alternative splicing. Hence, disruption of normal alternative splicing events during development results in the expression of misspliced forms of proteins that cannot support the functional requirements of a specific developmental stage. In many cases, this is due to frameshifting that leads to the loss of protein products. A few of the inherited genetic disorders are caused by defects in the regulation of alternative

splicing. Myotonic dystrophy (DM) is a good example of a disease caused by perturbation of developmentally regulated splicing events.

**Myotonic Dystrophy is an RNA-mediated Disease**

DM is a late onset neuromuscular disease that affects 1 in 8000 adults, making it the most common form of adult onset muscular dystrophy (1). Clinical manifestations include delayed muscle relaxation (myotonia), muscle weakness (myopathy), early-onset cataracts and cardiac conduction defects. As the name suggests, myotonia is a very unique clinical feature of this disease, which is often described as "stiffness" by patients and it makes DM distinctive from other type of muscular dystrophy.

At the molecular level, DM is caused by a CTG microsatellite expansion in the 3' untranslated region (UTR) of the DM protein kinase (*DMPK*) gene (DM1) and CCTG repeat expansions in the first intron of the *ZNF9* gene (DM2) (Fig. 1-1 *A*) (2, 3). In mitotic cells, the expansions of repeats involve mistakes during lagging-strand DNA replication. The formation of unusual DNA structures and DNA slippage lead to the repeat expansions in the nascent strand of DNA. For post-mitotic cells, DNA repair involving DNA synthesis is responsible for expansion mutations (Fig. 1-1 *B*) (4). Normal *DMPK* microsatellite lengths range from 5–37, whereas the DM1-affected population carries expansions from 50 to thousands of CTG repeats. In contrast, DM2 expansions can be massive with a disease range of 75 to >11,000 CCTG repeats. DM2 patients are generally mildly affected compared to DM1 with slight differences in the presentation of phenotypes however, overall they share very similar symptoms (5).

DM is an autosomal dominant disease, which means one mutant allele is enough to cause this genetically inherited disorder (1). In general, the number of repeats has a positive correlation with the severity of disease and a negative correlation with the age of onset. CTG repeats can expand greatly in the germline leading to genetic anticipation, which means that disease symptoms tend to be more severe and occur earlier in successive generations. Somatic mosaicism is also common, where expansion mutations can be significantly different in various tissues in a single individual. Even in the same tissue, repeats tend to get larger over time, which makes the disease highly variable and complex.

Several hypotheses, including DMPK haploinsufficiency or chromatin structural changes at the DM1 locus (*DMWD*, *DMPK* and *SIX5*) have been proposed to explain how microsatellite expansions in the non-coding region of a gene can cause a dominantly inherited genetic disease (6-8). These three genes are tightly clustered within an ~20 kb region with very short intergenic regions and the CTG expansion induces local chromatin structure changes and represses the expression of the genes at this locus. *Dmpk* knockout mice have been generated to directly test this idea and they develop cardiac conduction defects similar to DM and a late onset mild myopathy (9, 10). In addition, heterozygous loss of Six5 in mice leads to ocular central cataracts even though they are different than the type of subcapsular cataract that DM patients commonly develop (11). However, these hypotheses based on the DM1 locus fail to explain why a related expansion in a different gene located on another chromosome (DM2) results in similar phenotypes.

On the other hand, a series of recent studies support a toxic RNA gain-of-function hypothesis as the strongest disease model. In this model, mutant transcripts with CUG or

CCUG repeats are toxic because they fold into stable double stranded (ds) RNA hairpins that are not able to be exported out of nucleus and accumulate in nuclear RNA foci. These mutant RNAs disrupt RNA processing events in *trans* by altering the normal developmental regulation of alternative splicing (12-14) (Fig. 1-2). This idea is supported by the RNA fluorescence in situ hybridization (FISH) studies on DM1 skeletal muscle, which indicated that mutant *DMPK* transcripts are accumulated within nuclear foci whereas normal allele transcripts are exported out of nucleus and translated. In addition, a crystal structure of an 18-bp RNA containing six CUG repeats confirmed that CUG repeats RNA forms a pseudohelical structure similar to a standard A-form helix (15, 16). To directly test the hypothesis that CUG expansions in the pathogenic range are toxic independent of the gene context, transgenic mouse lines expressing 250 CTG repeats in the 3' UTR of the human skeletal actin (*HSA*) gene ($HSA^{LR}$) were generated (17). $HSA^{LR}$ transcripts formed multiple foci in skeletal muscle nuclei that are similar to those observed in DM patients. $HSA^{LR}$ mice also show severe hindlimb myotonia and dystrophic muscle features, demonstrating that CTG repeats alone are sufficient to recapitulate DM-like muscle pathology. Importantly, the expression level of the $HSA^{LR}$ transgene was proportional to the severity of the phenotype.

**Molecular Defects in DM: Perturbation of Alternative Splicing**

How do the mutant RNA transcripts retained in the nucleus exert a toxic effect? A key hypothesis in the field is that these mutant transcripts prohibit two RNA binding protein families, muscleblind-like (MBNL) and CUGBP1/ETR-3-like factors (CELF), from performing their cellular functions (7, 8, 18-20). Steady state levels of CUGBP1, which is

the most studied member of the CELF family of proteins, are increased in DM1 tissues due to hyperphosphorylation and stabilization through Protein Kinase C (PKC) activation (21-24). In contrast, MBNL activity is decreased because these proteins directly bind to the CUG repeats which leads to the loss of function due to sequestration (12, 25-27). A recent study reported that MBNL1 proteins form a ring-like structure and preferentially bind to the GC rich ds RNA hairpin containing a pyrimidine mismatch, which is similar to the structure of toxic CUG repeats (see Fig 1-2) (28). What are the cellular functions of these proteins? CELF and MBNL function antagonistically as alternative splicing factors such that CELF promotes inclusion of fetal exons, while MBNL promotes exclusion of fetal exons and/or inclusion of adult specific exons during development (18-20, 29). As a result, embryonic splicing patterns are retained in the DM patient cells because of increased CELF, and decreased MBNL, activity (19, 23). Consequently, the embryonic isoforms of many proteins lead to a functional failure in adult tissues.

In a previous study done in our lab, we tested the hypothesis that loss of MBNL1 function due to sequestration results in pathogenic effects by generating a mouse model in which the Mbnl1 isoforms that are capable of binding to CUG repeats were ablated ($Mbnl1^{\Delta E3/\Delta E3}$) (19). These mice recapitulate key features of DM including myotonia, subcapsular cataracts, cardiac conduction defects and missplicing of certain pre-mRNAs such as cardiac troponin T (Tnnt2), skeletal muscle troponin T (Tnnt3), insulin receptor (IR) and muscle specific chloride channel (Clcn1). This study suggests that loss of MBNL1 function is directly related to the pathogenesis of DM. In addition to *MBNL1*, humans and mice have two additional *MBNL* gene family members, *MBNL2* and *MBNL3*. MBNL

proteins share ~90% similarity in the RNA binding motif and all three MBNL proteins have similar splicing activities when ectopically expressed in cultured cells and they also colocalize with CUG repeat RNA in nuclear foci (18, 30). *Mbnl3* is mostly expressed embryonically and is not expressed in adult tissues however *Mbnl2* is highly expressed in multiple adult tissues (31). *Mbnl2* knockout mice were generated using available gene trapped alleles inserted into ES cells to test the functional role of the protein in vivo, but the phenotypes of these mice are mild to non-existent (32, 33). This result argues against a primary role of MBNL2 in DM pathogenesis. Cugbp1 overexpression transgenic mice were also generated to determine whether increased CUGBP1 function is sufficient to recapitulate DM. These mice display neonatal lethality when Cugbp1 expression is 4-6 fold above endogenous levels in heart and skeletal muscle (34) and they show abnormal muscle structure and missplicing of Tnnt2 and Clcn1 pre-mRNAs. These results support the possibility that elevated CUGBP1 activity, in addition to loss of MBNL activity, contributes to DM pathogenesis.

**MBNL1 Regulates Alternative Splicing during Post-natal Development**

In many cases of aberrant splicing events in DM, there is a failure to make the transition from the fetal to adult splicing pattern that results in a disruption of a developmentally regulated isoform switch. For example, aberrant splicing of the muscle-specific chloride channel (*CLCN1*) causes myotonia in DM, as it fails to switch to the adult splicing pattern during postnatal development (35, 36). In DM affected individuals, inclusion of exon 7a puts the mRNA out of frame and introduces a premature stop codon. These mRNAs are either degraded by the nonsense mediated decay (NMD) pathway or

produce truncated forms of the chloride channel. Since chloride channel proteins oligomerize into functional units, truncated protein isoforms generated by exon 7a inclusion exert a dominant-negative effect on the density of functional channels in the muscle membrane, consequently decreasing the ionic conductance (37, 38). Furthermore, morpholino antisense oligonucleotide (AON) targeting of the 3' splice site of *Clcn1* exon 7a reverses the defect of *Clcn1* alternative splicing, increases expression of the protein in the surface membrane and ultimately rescues myotonia in mouse models for DM ($HSA^{LR}$ and $Mbnl1^{\Delta E3/\Delta E3}$) which indicates that aberrant fetal exon inclusion of *Clcn1* is the molecular defect underlying the myotonic phenotype of DM (39).

While a specific subset of developmentally regulated pre-mRNAs is misregulated in DM, this perturbation of splicing regulation seems to affect many genes. In a recent study that examined splicing in skeletal muscle of $Mbnl1^{\Delta E3/\Delta E3}$ mice using splicing sensitive microarrays, more than 200 novel splicing events were found altered. (Du et al. *in press*). Also, there was a striking concordance of missplicing events between $HSA^{LR}$ and $Mbnl1^{\Delta E3/\Delta E3}$ muscles, which suggests that loss of MBNL1 is the primary event for splicing defects in DM muscle pathology.

Although loss of MBNL1 protein seems to play a major role in DM pathogenesis, there are other RNA binding proteins that are implicated in DM pathogenesis such as hnRNP H and the transcription factor Sp1 (40, 41), even though their involvement in DM pathogenesis seems to be limited. HnRNP H proteins are colocalized with mutant transcripts in the nuclear foci of DM patient cells by RNA fluorescence in situ hybridization (RNA-FISH) staining, which may cause decreased activity of these proteins.

HnRNP H has also shown to interact with MBNL1 and CUGBP1 to regulate insulin receptor (IR) splicing, which is misregulated in DM patients (21).

**Therapeutic Approaches for DM**

We hypothesized that dysregulation of developmental splicing events by decreased MBNL1 activity plays a major role in DM pathogenesis, rather than increased CUGBP1 activity or decreased hnRNP H activity. Thus, increasing nuclear MBNL1 availability should be sufficient to reverse the splicing events and the DM muscle phenotype including myotonia and muscle histopathology. This study provides a proof-of-principle that MBNL1 loss-of-function is a primary pathogenic event in DM.

This study will also examine the possibility of using a gene therapy approach to upregulate MBNL1 proteins as a therapeutic treatment. Many drugs have been used to treat DM patients, including selenium, vitamin E, baclofen, nifedipine, creatine monohydrate and testosterone, but all have failed to show significant clinical benefits (42). Other compounds, including DHEA-S and bioflavonoids, are able to ameliorate cytotoxicity induced by CTG repeat tracts in a cell culture system but the mechanism that triggers this beneficial effect is unclear. Treatment for DM so far has been focused on relieving muscle degeneration rather than resolving disease pathogenesis at the molecular level (43).

New therapeutic approaches have emerged recently and they have proven to be very effective, at least in mouse models. Treatment of AON containing $(CAG)_{25}$ in the $HSA^{LR}$ mouse blocks the interaction of Mbnl1 with toxic CUG RNA and leads to the correction of defective Clcn1 alternative splicing and myotonia (44). In similar manner, administration of 2'-O-methyl-phophorothioate-modified $(CAG)_7$ AON in a DM mouse model carrying a

human DMPK transgene with a CTG repeat expansion also significantly reduces aberrant alternative splicing (45). Efforts to screen small molecules that can disrupt MBNL1 binding to CUG repeats is also ongoing and one of these potential drugs, pentamidine, is effective in a cell culture model and partially rescues missplicing in the *HSA*$^{LR}$ mouse (46).

In this study, we used recombinant adeno-associated virus (rAAV) mediated gene transfer to upregulate Mbnl1 protein since rAAV is non-pathogenic which makes it an attractive vector for gene therapy (47). Early phase clinical trials using rAAV have been performed for cystic fibrosis (CF) and hemophilia B (48-51). Results were positive, generally indicating lack of vector-mediated toxicity, efficient rates of DNA transfer, and transient decreases in pathogenic effects.

In this study, we address the role of MBNL1 sequestration *in vivo* by using adeno-associated virus (AAV)-mediated transduction to overexpress the protein in *HSA*$^{LR}$ skeletal muscle. Our results demonstrate that elevated expression of Mbnl1 alone is sufficient to rescue the myotonia and aberrant splicing of specific gene transcripts that are characteristic manifestations of DM skeletal muscle.

## Results

### Selection of the Mbnl Isoform for Overexpression in Skeletal Muscle

There are three *MBNL* genes in humans and mice (12, 30). They all have two pairs of zinc-knuckle-like (CCCH, C3H) motifs (4XC3H proteins) that are required for RNA binding and share 90% sequence similarity. Co-transfection analysis of HEK293 and HeLa cells with minigene splicing reporters and human MBNL expression plasmids demonstrates that all three MBNL proteins (MBNL1, MBNL2, and MBNL3) promote fetal exon

exclusion to a similar extent (18). Nevertheless, we chose Mbnl1 for AAV-mediated overexpression in *HSA*$^{LR}$ skeletal muscle primarily because transgenic *HSA*$^{LR}$ and *Mbnl1*$^{\Delta E3/\Delta E3}$ knockout models for DM both develop myotonia, distinctive morphological changes to muscle structure, and remarkably similar adult missplicing patterns (17, 19, 33). Also recent data showed that two *Mbnl2* genetrap mice fail to show dramatic dystrophic changes in muscles (32, 33). Further, expression of Mbnl3 is primarily expressed during embryonic skeletal muscle development so it is unlikely that this isoform regulates splicing during postnatal development (31).

Since loss of Mbnl1 function and expression of CUG repeat expansions causes similar muscle phenotypes, we expected to see a rescue of pathogenic phenotypes upon Mbnl1 overexpression either by upregulation of free Mbnl1 protein in the nucleus or by increased Mbnl1 binding to dsCUG RNA thereby releasing the sequestered endogenous proteins. The later possibility is supported by a fluorescence recovery after photobleaching (FRAP) study on DM1 fibroblasts that reported relatively rapid exchange rates between MBNL proteins within ribonuclear foci and the surrounding nucleoplasmic pool (52).

Another question focused on which Mbnl1 isoform should be overexpressed in *HSA*$^{LR}$ skeletal muscle. The mouse *Mbnl1* gene encodes at least 14 isoforms that use two different initiation codons (19). Isoforms that initiate in exon 3 contain four copies of C3H (4XC3H) whereas the isoforms that use the exon 4 initiation codon contain only two C3H motifs (2XC3H) (Fig 2-1) (12, 28, 53). To determine the most effective isoform for AAV-mediated muscle expression, we identified the predominant Mbnl1 isoforms expressed in adult mouse skeletal muscle. Because deletion of exon 3 in the mouse was sufficient to

cause the multisystemic DM-like phenotype in *Mbnl1*$^{\Delta E3/\Delta E3}$ mice (19), we used primers positioned in *Mbnl1*exons 3 and 13. The cDNAs from mouse postnatal day (P) 28 quadriceps were amplified to determine the coding sequences for the isoforms initiating in exon 3.This time point was chosen because the postnatal developmental transition of Mbnl1 isoforms occurs between P2 and P20 (33). P2 hindlimb cDNAs were also analyzed to compare neonatal isoforms to their adult counterparts. For each time point, complete DNA sequences of 72–81 Mbnl1 cDNA clones were determined. At P2, the major Mbnl1 4XC3H isoforms are 41, 40, and 35 kDa whereas by P28 the 41-kDa isoform is no longer expressed (Fig. 1-3 *A*). Seven additional isoforms (43, 42, 38, 37, 36, 36*, and 32) were also identified at significantly lower levels. Immunoblot analysis using the A2764 polyclonal antibody directed against the Mbnl1-specific carboxyl-terminal peptide confirmed that the major adult protein in three different skeletal muscles (tibialis anterior, gastrocnemius, and quadriceps) was of 40 kDa, whereas the major isoforms in cerebellum, heart and lung are slightly larger (Fig. 1-3 *B*).

We pursued the possibility of using the Mbnl1 41-kDa isoform (Mbnl1/41) for AAV-mediated transduction because a previous study confirmed that MBNL1/41 has a high affinity for a CUG repeat expansion RNA [$(CUG)_{54}$] with a *K*d of 5.3 nM (28). To determine the splicing activity of Mbnl1/41 we used a HEK293T co-transfection assay to compare splicing activities of various Mbnl1 isoforms and unrelated RNA-binding proteins. Fast skeletal muscle troponin T (Tnnt3) was selected as the minigene reporter because splicing of its fetal exon is very sensitive to Mbnl1 levels *in vivo* (19, 28). For protein expression, GFP fusion expression plasmids were used so that the transfection efficiency

could be monitored readily. Although overexpression of other RNA-binding proteins, including splicing factors hnRNP A1 and CUGBP1 failed to alter the F exon-splicing pattern, all Mbnl1 isoforms tested significantly enhanced F exon skipping (Fig. 1-4). Mbnl1 41- and 40-kDa isoforms showed the highest Tnnt3 F exon skipping activity. Importantly, there was no difference in the splicing activities of these 4XC3H isoforms in this assay with ≈85% Tnnt3 fetal exon exclusion in cells expressing either GFP-Mbnl1/40 or GFP-Mbnl1/41.

**Reversal of Myotonia in *HSA*$^{LR}$ mice after Overexpression of Mbnl1**

For Mbnl1 overexpression, we selected the tibialis anterior (TA) muscle because it is relatively small, readily accessible without surgery, and efficiently transduced by AAV (54). Four-week-old *HSA*$^{LR}$ mice were injected with $1 \times 10^{11}$ vector genomes (vg) in the right TA with AAV2/1 (AAV2 ITR in an AAV1 capsid) modified to express the myc-tagged Mbnl1 41-kDa isoform (AAV2/1-mycMbnl1/41). Relative levels of endogenous 40-kDa versus exogenous mycMbnl1/41 expression were assessed by immunoblotting. At 23 weeks after injection, the mycMbnl1/41 protein was present in injected, but not in uninjected TA muscles (Fig. 1-5 *A*). Compared with the uninjected TA, the level of the endogenous 40-kDa protein in the injected muscle was reduced ~20% when normalized to Gapdh. Despite this reduction, there was an overall 2-fold increase in Mbnl1 protein due to AAV2/1-mycMbnl1/41 expression. Because of the high expression level of the *HSA*$^{LR}$ transgene, numerous discrete ribonuclear foci containing Mbnl1, which colocalizes with $(CUG)_{250}$ RNA (27), were detectable in transgenic myonuclei (Fig. 1-5 *B*). In contrast, Mbnl1 was more diffusely distributed in the nucleus after AAV-mediated overexpression,

suggesting that a subpopulation of this splicing factor was no longer sequestered in these foci.

Electrical myotonia is a prominent pathological feature of both human DM and mouse *HSA*$^{LR}$ skeletal muscle. Electromyography revealed a striking reduction of myotonia specifically in the *HSA*$^{LR}$ -injected TA by 4 weeks after injection and a complete absence of myotonic discharges at 23 weeks (Fig. 1-6 *A*). By 43 weeks after injection, muscle hyperexcitability was again detectable in some mice, whereas myotonia present in both uninjected *HSA*$^{LR}$ TA and gastrocnemius muscles was unaffected at all time points assayed, which indicates that overexpression of Mbnl1 is injection site specific.

Myotonia in DM results from missplicing of the major skeletal muscle chloride channel CLCN1 in adults, which results in loss of functional membrane-associated chloride channels. Clcn1 protein levels were reduced markedly in *HSA*$^{LR}$ muscle compared with control FVB muscle levels. After Mbnl1 overexpression, Clcn1 was restored to near wild-type levels in injected TA muscles at 23 weeks after injection (Fig. 1-6 *B* and *C*). Mouse *HSA*$^{LR}$ muscles show DM-relevant morphological abnormalities, including centralized nuclei, split fibers, and fiber size heterogeneity in the absence of significant muscle necrosis (17). In contrast to the myotonia, these abnormalities were still present in injected TA muscles at all time points examined (Fig. 1-6 *E* and *F*).

**Reversal of Myotonia Correlates with Rescue of Missplicing of Specific Developmentally Regulated Exons**

Since myotonia was eliminated by 23 weeks after injection of AAV2/1-mycMbnl1/41, we characterized alternative splicing of fetal exon of Clcn1 in FVB, *HSA*$^{LR}$, and AAV2/1-mycMbnl1/41-injected mice. Whereas in wild-type FVB mice, exons 6, 7,

and 8 are spliced directly together, exon 7a is included in *HSA*$^{LR}$ muscle (Fig. 1-7). As expected, overexpression of Mbnl1 reversed this splicing defect by promoting Clcn1 exon 7a exclusion to the normal adult pattern.

Another pre-mRNA that is misspliced in DM is Ldb3/Cypher/Zasp, which encodes a striated muscle PDZ-LIM domain protein that localizes to the Z line and interacts with α-actinin 2. Although *Cypher* expression is not essential for sarcomerogenesis or Z line function, Cypher proteins are important for normal muscle function and *Cypher* knockout mice die perinatally because of severe congenital myopathy. Cypher is misspliced in DM1 and DM2 muscle (33, 55). Interestingly, human *CYPHER*/*ZASP* mutations have been linked to a novel autosomal dominant muscular dystrophy (56). During development, the embryonic Cypher isoform (Cypher1S) is replaced postnatally by Cypher 3S by skipping of Cypher exon 11. As expected, normal FVB adults showed exon 11 skipping, whereas *HSA*$^{LR}$ mice recapitulated the wild-type neonatal pattern with equivalent levels of exon 11 inclusion and exclusion. At 23 weeks after injection, the adult Cypher splicing pattern was restored in AAV2/1-mycMbnl1/41-injected *HSA*$^{LR}$ TA muscles, with the majority of mRNAs excluding exon 11.

Intracellular skeletal muscle calcium homeostasis is regulated by the sarcoplasmic reticulum (SR) proteins, ryanodine receptor 1 (Ryr1) and SR/endoplasmic reticulum $Ca^{2+}$ ATPase (Serca) 1. Whereas Ryr1 releases $Ca^{2+}$ from the SR, Serca is the skeletal muscle SR $Ca^{2+}$ reuptake pump. A previous study demonstrated that Serca1 exon 22 is included in adult muscle but excluded in neonatal, as well as adult DM1 and mouse *HSA*$^{LR}$ muscle (57). In agreement, exon 22 was predominantly included in FVB adult Serca1 mRNA

whereas the neonatal pattern of ~50% inclusion was observed in *HSA*$^{LR}$ adult TA. Overexpression of Mbnl1 after AAV2/1-mycMbnl1/41 injection led to a significant increase in exon 22 inclusion and near-normal adult Serca1 splicing.

Fast skeletal muscle troponin T (TNNT3) is the subunit of the troponin complex that binds to tropomyosin. Although TNNT3 contains several alternatively spliced exons (4, 6, 7, 8, F, 16, and 17), only F exon splicing is altered in DM (19). The requirement for F exon inclusion in fetal muscle is unclear. In *HSA*$^{LR}$ adult muscle, the F exon is included together with different combinations of alternatively spliced exons 4–8, which yields multiple cDNAs containing the F exon, whereas the F exon is excluded from normal FVB TA adult muscle. In agreement with the hypothesis that Mbnl1 is the primary regulator of this exon, nearly all F exon inclusion was eliminated in injected TA muscle.

In contrast, alternative splicing of Capzb exon 8 and Itgb1 exon 17, two pre-mRNAs whose splicing is not affected by the DM expansion mutation (33), were unaffected in *HSA*$^{LR}$ and AAV-transduced mice compared with FVB controls at all time points. Control TA injections with AAV expressing only GFP driven by the same CBA promoter (AAV2/1-GFP) also showed no effect in this model and failed to reverse the splicing pattern of Serca1 and Tnnt3, suggesting rescue of DM associated phenotypes after AAV2/1-mycMbnl1/41 injection is Mbnl1 protein specific event.

Because myotonia showed gradual rescue from the 4 week to 23 week time points followed by recurrence at 43 weeks, we speculated that we would see the corresponding reversal of alternative splicing of the target pre-mRNAs. We examined Serca1 exon 22 splicing patterns at each of the time points (4, 12, 23 and 43 weeks after injection) and as

we expected, a higher level of exon 22 inclusion was observed at 23 weeks after injection compared to 4 or 12 weeks (Fig. 1-8). The result from the 43 week time point was comparable to 23 weeks. A similar trend was observed for the reversal of Tnnt3 missplicing. The degree of rescue in missplicing also correlated with the expression level of ectopic mycMbnl1/41 expression in myonuclei. We quantified myonuclei expressing myc-tagged Mbnl1 after AAV2/1-mycMbnl1/41 injection by counting myc-positive and myc-negative nuclei using anti-myc monoclonal antibody 9E10 (Fig. 1-9). As expected from the splicing assay, the percentage of myonuclei expressing mycMbnl1/41 was higher for 23-week postinjection time point compared to 4-week, which provides explanation for more complete rescue of myotonia and missplicing at 23 weeks.

**Systemic Delivery of Mbnl1 in Neonate Poly(CUG) Mice**

Whereas direct muscle injection of AAV2/1-mycMbnl1/41 effectively demonstrated a primary role of MBNL1 in myotonia and missplicing in DM, systemic intravenous transduction is a more useful approach for balanced and uniform expression of a transgene since DM skeletal muscles are systemically compromised. This approach will also enable us to analyze the change in muscle histopathology more accurately in the absence of any structural changes resulting from injury induced by direct injection. Therefore, we tested if Mbnl1 systemic overexpression would rescue the myotonia and RNA missplicing in the multiple skeletal muscles of the same mouse model using systemic gene transfer. We chose AAV2/8 for systemic delivery because previous studies have indicated that AAV2/8 is superior to AAV2/1 for the transduction of skeletal muscles following intravenous injection due to its ability to cross the blood vessel barrier (58). Before we proceeded to systemic

injection, we first confirmed that AAV2/8-mycMbnl1/41 was able to switch splicing after direct muscle injection.

AAV2/1-mycMbnl1/41 and AAV2/8-mycMbnl1/41 ($1 \times 10^{10}$ vg each) were delivered to TA muscle of *HSA*$^{LR}$ mice to compare the efficacy of splicing reversal of Serca1 exon 22. We chose this amount of virus, which is 10 fold less than what we used earlier, because we expected $1 \times 10^{11}$ vg of AAV-Mbnl1 to saturate binding sites on CUG repeats and prevent us from comparing the efficiency of different types of virus. Four weeks after injection, splicing patterns for alternative exon 22 were tested. As we expected, both AAV2/1 and AAV2/8-mycMbnl1/41 were able to rescue Serca1 missplicing. Indeed, AAV2/8-mycMbnl1/41 showed activity compared to AAV2/1-mycMbnl1/41. Because purified AAV2/8-mycMbnl1/41 was active in splicing, we proceeded with systemic injections of *HSA*$^{LR}$ poly(CUG) mice.

One day old anesthetized *HSA*$^{LR}$ mice were administered with $2.5\text{-}5 \times 10^{11}$ vg of AAV2/8-mycMbnl1/41 intravenously via the superficial temporal vein. Unfortunately, all mice died within 10 days of injection, suggesting that AAV2/8-mycMbn1/41 expression in neonatal mice is toxic. We analyzed autopsy muscle RNA samples and found the partial adult splicing pattern of Serca1 exon 22 in the injected muscle 6 days of post- injection. This result indicates that inappropriate inclusion of the adult, and/or exclusion of the fetal, exon may underlie lethality after Mbnl1 overexpression in neonates. We also examined expression levels of Mbnl1 transcripts by RT-PCR in multiple tissues and saw very high expression in the heart and liver, in agreement preferred transduction tropism for AAV8 (58). We speculate that inappropriate high expression of Mbnl1 in these tissues results in

aberrant alternative splicing that leads to early lethality in AAV2/8-mycMbnl1/41 injected *HSA*$^{LR}$ mice.

## Discussion

We have shown that AAV-mediated gene transfer of Mbnl1/41 is able to rescue DM-associated myotonia and missplicing events in a poly(CUG) mouse model for DM. Our initial concern was that CUG repeat expression driven by the *HSA* promoter is too high and it would be impossible to saturate Mbnl1 binding sites on CUG transcripts in myonuclei. However two fold overexpression of Mbnl1 was sufficient to rescue myotonia and missplicing of Clcn1 as well as other aberrant alternative splicing events in poly(CUG) muscle. Interestingly we observed that endogenous Mbnl1/40 level was downregulated by ~20% upon ectopic overexpression of mycMbnl1/41, which suggests a possible regulatory mechanism to maintain a consistent level of Mbnl1. Mbnl1 has a long 3' UTR which contains *cis* regulatory elements for mRNA translation and turnover and it is tempting to speculate that Mbnl1 binds to its own 3' UTR to repress translation or regulate stability which results in downregulation of the protein. Since Mbnl2 and Mbnl3 have similar RNA binding domains, it is also possible that Mbnl1 overexpression affects the stoichiometry of other Mbnl gene family members in the nucleus and regulates the endogenous pool of Mbnl1 indirectly.

After two-fold overexpression in the TA muscle in the poly(CUG) mouse, Mbnl1 proteins were more diffusely distributed throughout the nucleoplasm, suggesting that a subpopulation of Mbnl1 proteins are no longer sequestered in nuclear foci and free Mbnl1 proteins promote the reversal of myotonia and missplicing. It is also possible that ectopic

expression of Mbnl1 releases other proteins such as Mbnl2 and hnRNP H for phenotypic reversal. However, we prefer the idea that increased Mbnl1 in the nucleoplasm plays a major role in reversing the disease-associated phenotypes for the following reasons. First, the *Mbnl1* knockout mouse shows more disease-associated phenotypes compared to *Mbnl2* genetrap mice. Second, exon array anlaysis of $HSA^{LR}$ and $Mbnl1^{\Delta E3/\Delta E3}$ muscle shared >80% similarity in specific missplicing events, suggesting that Mbnl1 loss of function is able to explain the majority of RNA splicing changes induced by toxic CUG repeats. Third, the role of hnRNP H in DM pathogenesis seems limited because there are only a few splicing targets affected in DM that have been shown to be regulated by hnRNP H *in vitro*. On the other hand, it is tempting to speculate that Mbnl2 interacts with Mbnl1 to cause disease phenotypes considering that Mbnl1 proteins form oligomeric structures on CUG repeats via their C-terminal residues. This idea was tested by crossing *Mbnl1* and *Mbnl2* knockout mice and *Mbnl1/Mbnl2* double knockout mice were embryonic lethal (Unpublished data, Thornton et al) suggesting possible synthetic effects from loss of function of both these proteins. It would be interesting to test whether these proteins form a heterotypic complex which regulates alternative splicing during development.

Even though we observed significant reduction of myotonia at all time points tested (4, 12, 23 and 43 weeks after injection), reversal of myotonia was significant at 23 weeks post-injection and correction of missplicing was more complete at this time point as well. Complete rescue at 23 weeks seems to be related to higher ectopic expression of mycMbnl1 at this time point (Fig. 1-9). Generally, AAV2/1 reaches maximum expression ~8 weeks after administration, and additional time is required to replace existing protein isoforms.

Therefore, maximum rescue of disease phenotypes at 23 weeks after injection seems to fit to our current knowledge of the AAV expression profile. Recurrence of myotonia could be due to transgene loss caused by myofiber turnover which is a characteristic feature of *HSA*$^{LR}$ mouse muscle. In addition, muscle cell turnover is initiated by the activation of satellite cells, myoblasts proliferation and the fusion of the latter cells to existing myofibers. Therefore insufficient transduction of muscle satellite cells by AAV2/1-mycMbnl1/41 could result in transgene loss of transgene in newly synthesized muscle cells.

Histopathology of muscle cells, such as centralized nuclei, is another DM-associated phenotype in *HSA*$^{LR}$ mice. Unlike myotonia, we were not able to rescue the centralized myonuclei phenotype. Following AAV2/1-mycMbnl1/41 administration, myofibers seem to have even more centralized nuclei. It is possible that the Mbnl1 level was not sufficient to rescue histopathology even though all of the tested alternative splicing patterns reverted to near normal adult patterns. We prefer the alternative that muscle pathology in the poly(CUG) mouse resulted not only from the missplicing events due to Mbnl1 sequestration but also from the perturbation of other regulatory pathways due to loss of additional factors, such as Mbnl2. This idea is supported by a recent study that showed poly(CUG) mice display a transcriptional dysregulation that cannot be explained by loss of Mbnl1 and may be attributable to Mbnl2 loss-of-function. Transcription of a group of genes involved in the regulation of extracellular matrix structure and function was misregulated in *HSA*$^{LR}$, but not in *Mbnl1*$^{\Delta E3/\Delta E3}$, mouse muscle. Since Mbnl2 has been proposed to have a function in mRNA transport and localization (59), it would be interesting to perform genetic complementation of *Mbnl2* in poly(CUG) mice to see if Mbnl2 overexpression will

ameliorate muscle pathology in f these mice. In addition, combinational overexpression of Mbnl1 and Mbnl2 can also be performed to see if this combination completely rescues muscle histopathology.

An alternative explanation for the failure to rescue muscle histopathology is that AAV2/1-mycMbnl1/41 administration triggers an immune response and accelerates the regeneration of myofibers due to expression of an antigen. This idea is supported by the result that control AAV2/1-GFP administration in TA muscle of $HSA^{LR}$ showed the same histopathological changes, such as increased myofibers with centralized nuclei. Injection of tolerized untagged Mbnl1 may be able to solve this issue. However systemic delivery will be critical to test the idea because direct muscle injection leads to a physical injury at the injection site.

We made an attempt to deliver AAV2/8-mycMbnl1/41 systemically in neonate poly(CUG) mice to rescue myotonia and missplicing in multiple muscle tissues. All of the injected mice showed early lethality, which suggests possible toxic effects of Mbnl1 overexpression during the neonatal period. While we believe this result reflects the perturbation of development signals by improper temporal and spatial expression of Mbnl1, we cannot exclude the possibility that toxic effects of AAV capsid proteins in the heart and liver as possible causes of death even though previous studies using AAV in neonate mice argue against this possibility (58). In the future, we will change our strategy and deliver AAV2/8-Mbnl1 to adult mice.

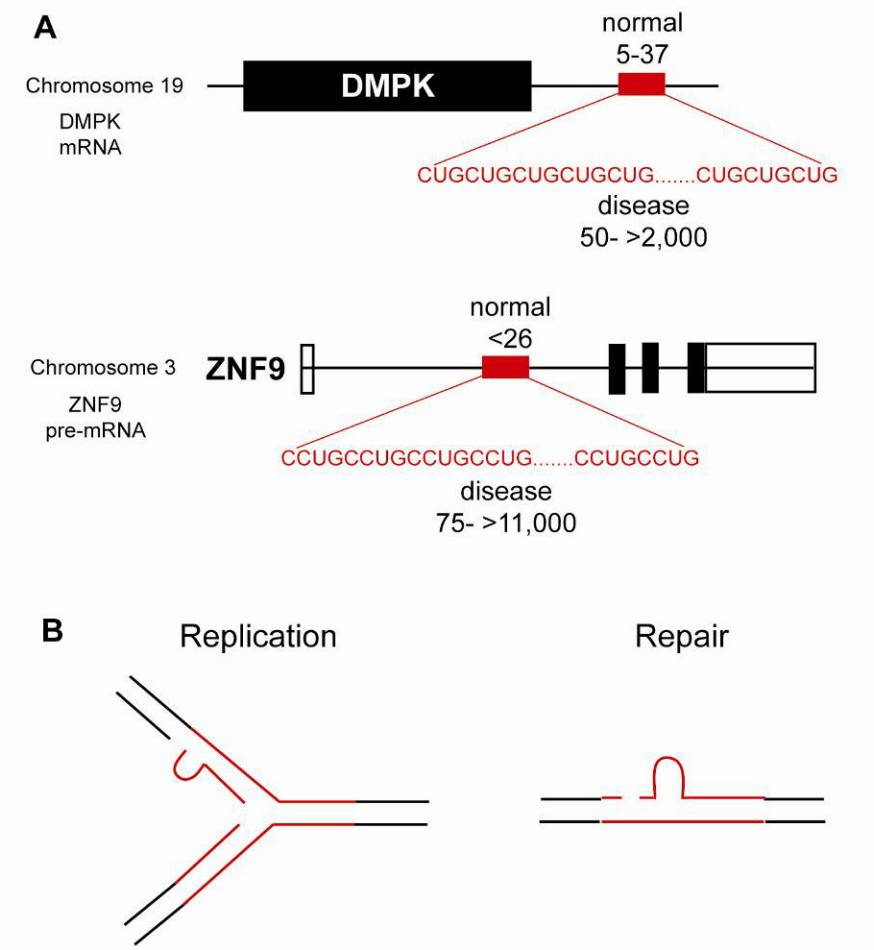


Figure 1-1. RNA-mediated pathogenesis in myotonic dystrophy (*A*) DM1 is cause by a CTG repeat expansion in the 3' UTR of the *DMPK* gene. Mutant DMPK mRNA (black line) with coding region (black box labeled DMPK) and CUG expansions in the 3' UTR are indicated. DM2 is caused by a CCTG repeat expansion in the first intron of *ZNF9*. Non-coding (open boxes) and coding exons (black boxes) of mutant *ZNF9* gene (black line) are indicated. (B) Microsatellite expansions in DM are associated with mistakes during DNA replication and repair. C(C)TG repeats form unusual hairpin structures (red line) and lead to the expansion mutation in nascent DNA strands.

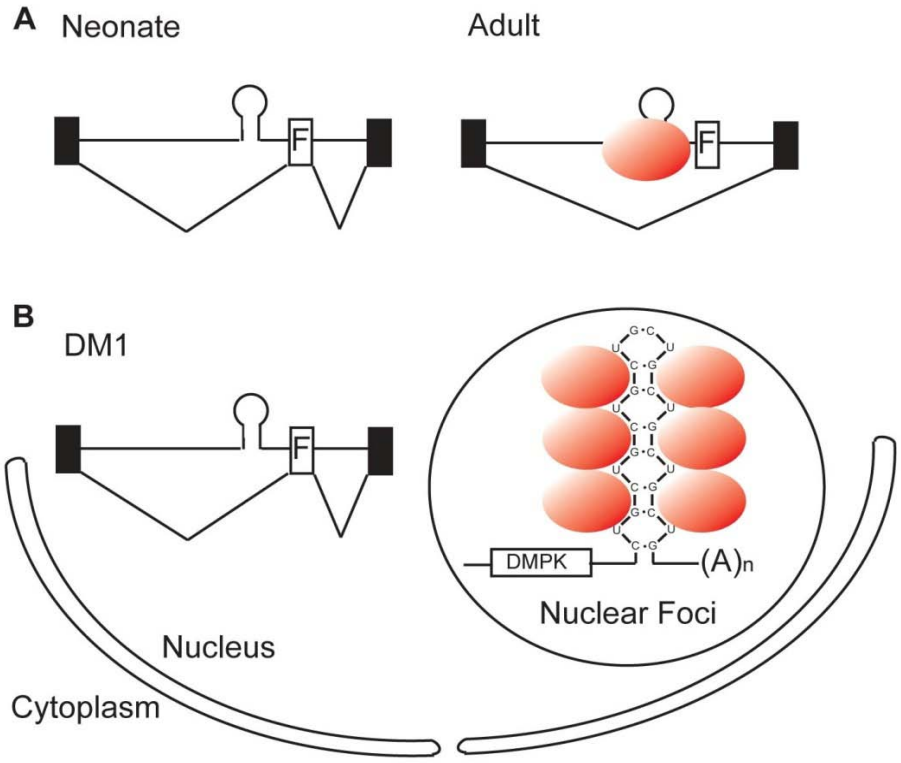


Figure 1-2. Loss-of-function of alternative splicing factor MBNL1 in myotonic dystrophy. (A) MBNL1 promotes fetal exon skipping by binding to the 3' splice site of the exon. In normal neonatal tissues, MBNL1 is located cytoplasm and not available in the nucleus, which results in the inclusion of the fetal exon. In adult tissues, MBNL1 (red oval) binds to the target pre-mRNA promoting exclusion of the fetal exon. (B) In DM1, the fetal splicing pattern persists in the adult due to sequestration of MBNL1 by CUG expansion RNA. The RNA-protein complex accumulates in nuclear foci.

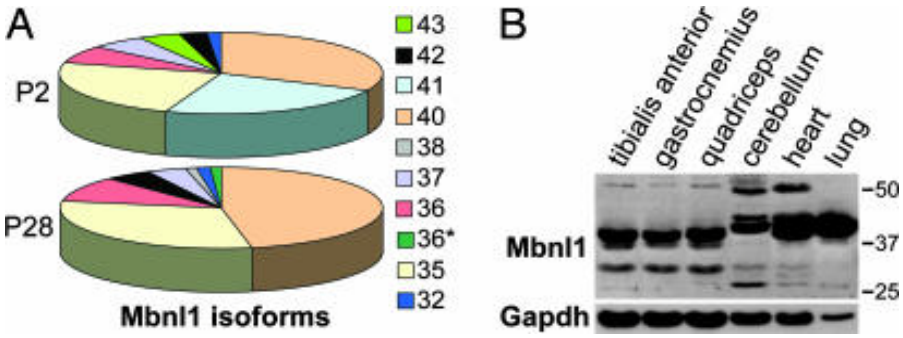


Figure 1-3. Expression of Mbnl1 isoforms in skeletal muscle. (*A*) Distribution of Mbnl1 isoforms in neonatal (P2) and P28 muscle. Ten hindlimb muscle isoforms were identified by RT-PCR followed by cDNA sequencing. Isoforms (color coded) are as follows (in kDa): 43, lime green; 42, black; 41, turquoise; 40, orange; 38, purple; 37, light blue; 36, red; a 36 spliced variant (36*, dark green); 35, yellow; and 32, blue. (*B*) The major Mbnl1 protein in adult skeletal muscle is 40 kDa. Immunoblot analysis was performed on three skeletal muscles (tibialis anterior, gastrocnemius, and quadriceps), cerebellum, heart, and lung by using either anti-Mbnl1 or anti-Gapdh (loading control). Reprinted from *Reversal of RNA missplicing and myotonia after muscleblind overexpression in a mouse poly(CUG) model for myotonic dystrophy*; Kanadia RN, Shin J, Yuan Y, Beattie SG, Wheeler TM, Thornton CA, Swanson MS; Copyright 2006 Proc Natl Acad Sci U S A.

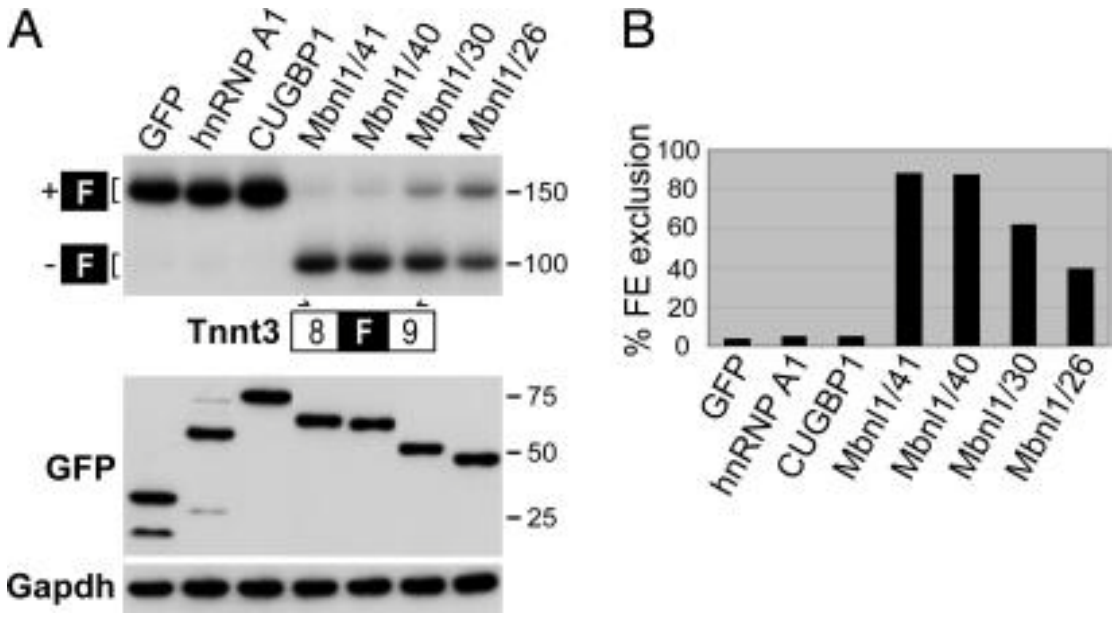


Figure 1-4. Mbnl1 isoforms with the 4XC3H motif has a higher splicing activity. (*A Upper*) RNA splicing in HEK293T cells transfected with a Tnnt3 minigene reporter and protein expression plasmids containing GFP, GFP-hnRNP A1 and GFP-CUGBP1, and GFP-Mbnl1 4XC3H (Mbnl1/40 and Mbnl1/41) and 2XC3H (Mbnl1/30 and Mbnl1/26) isoforms. (*A Lower*) An immunoblot of GFP fusion protein expression showing equivalent expression levels for GFP and GFP-fusion proteins after transfection. Protein loading control is Gapdh. PCR primers (arrows) are located in Tnnt3 exons 8 and 9 (open boxes) bordering the alternatively spliced fetal (F) exon (filled box). (*B*) Phosphorimager quantification of percent fetal exon (FE) exclusion from the PCR data shown in *A*. Reprinted from *Reversal of RNA missplicing and myotonia after muscleblind overexpression in a mouse poly(CUG) model for myotonic dystrophy*; Kanadia RN, Shin J, Yuan Y, Beattie SG, Wheeler TM, Thornton CA, Swanson MS; Copyright 2006 Proc Natl Acad Sci U S A.

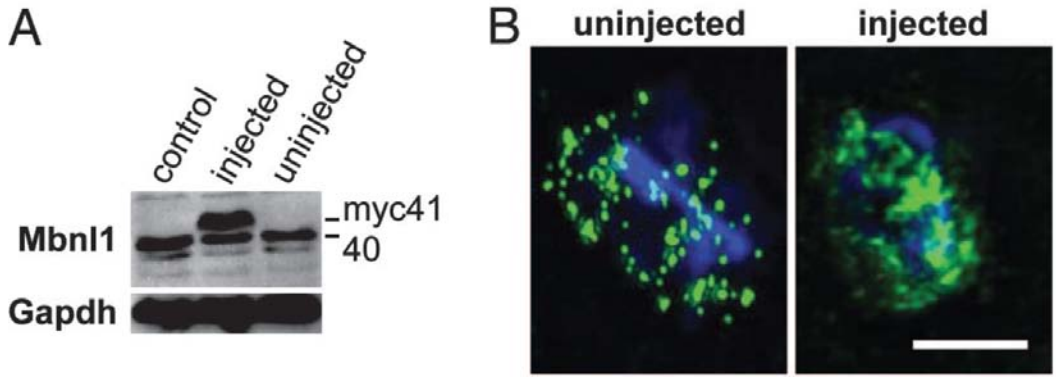


Figure 1-5. Overexpression of Mbnl1 leads to free Mbnl1 protein in nucleoplasm. (*A*) Mbnl1 is overexpressed after AAV2/1-mycMbnl1/41 transduction of TA muscle. TA muscles (23 weeks after injection) were dissected from either uninjected (control) or injected $HSA^{LR}$ mice (both injected and uninjected muscles are shown) and total protein immunoblotted with anti-MBNL1 antibody. Gapdh is the protein loading control. (*B*) Distribution of Mbnl1 protein in transverse sections of skeletal muscle. Shown are max-value projections of deconvolved images obtained under identical exposure settings. $HSA^{LR}$ sections from uninjected (*Left*) and injected (*Right*) TA muscles were stained by using the anti-Mbnl1 antibody. (Scale bar: 5 μm.) Reprinted from *Reversal of RNA missplicing and myotonia after muscleblind overexpression in a mouse poly(CUG) model for myotonic dystrophy*; Kanadia RN, Shin J, Yuan Y, Beattie SG, Wheeler TM, Thornton CA, Swanson MS; Copyright 2006 Proc Natl Acad Sci U S A.

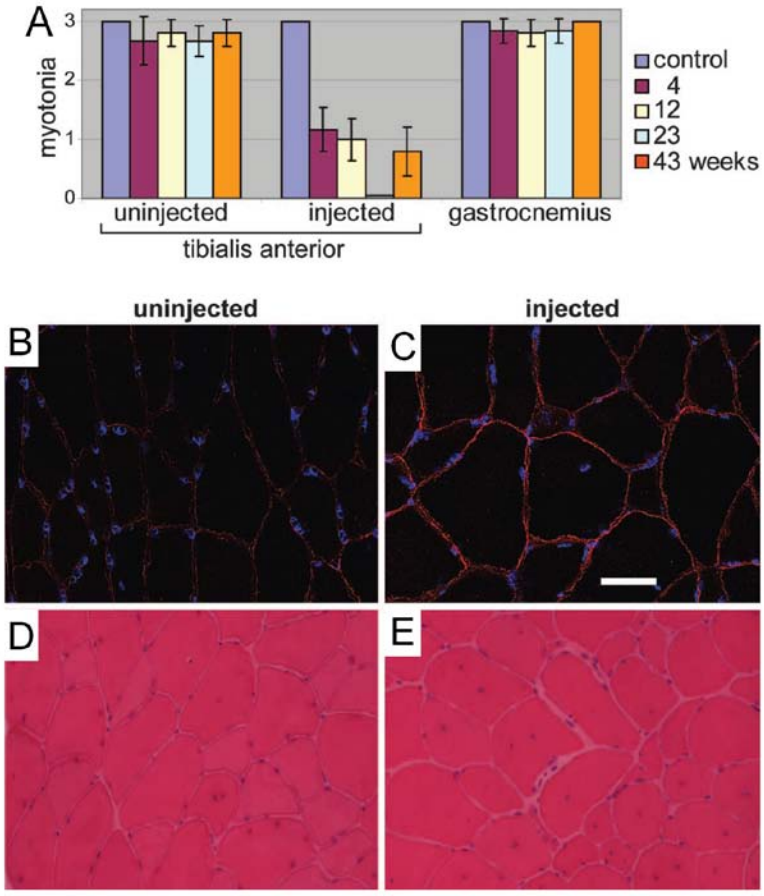


Figure 1-6. Reversal of myotonia following Mbnl1 overexpression (*A*) Myotonia was assessed by electromyography on $HSA^{LR}$ mice injected in the right TA. The uninjected left TA and gastrocnemius muscles also were tested. The electromyography scale is as follows: 0, no myotonia; 1, occasional myotonic discharge in <50% of needle insertions; 2, myotonic discharge with >50% of insertions; 3, myotonic discharge with nearly all insertions. Uninjected control and injected $HSA^{LR}$ mice were tested at 4 (purple), 12 (yellow), 23 (turquoise), and 43 (orange) weeks after injection. (*D* and *E*) Restoration of Clcn1 protein levels in myofiber membranes after Mbnl1 overexpression. Clcn1 protein levels were detected in uninjected (*D*) and injected (*E*) transverse muscle sections at 23 weeks after injection by using an anti-Clcn1 polyclonal antibody (red). DNA distribution is shown by DAPI staining (blue). (Scale bar: 10 μm.) (*F* and *G*) Muscle histology (H&E staining) of muscle sections from uninjected (*F*) and injected (*G*) TA at 43 weeks after injection. Reprinted from *Reversal of RNA missplicing and myotonia after muscleblind overexpression in a mouse poly(CUG) model for myotonic dystrophy*; Kanadia RN, Shin J, Yuan Y, Beattie SG, Wheeler TM, Thornton CA, Swanson MS; Copyright 2006 Proc Natl Acad Sci U S A.

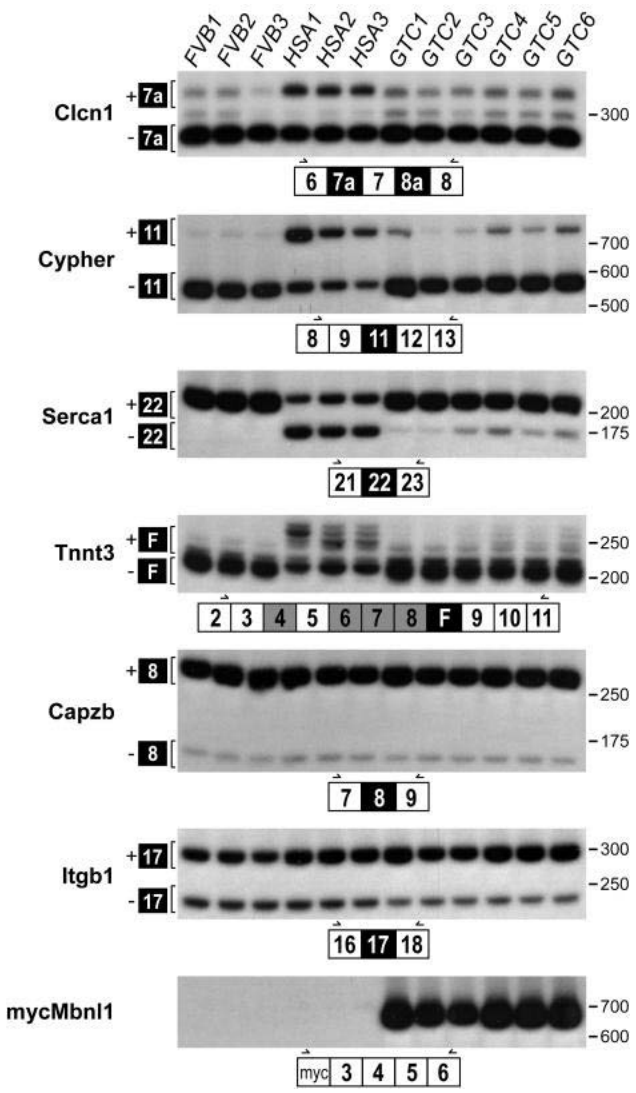


Figure 1-7. Mbnl1 overexpression promotes adult splicing patterns. RT-PCR splicing assays of uninjected FVB/n and *HSA*$^{LR}$ (three mice each) or AAV2/1-mycMbnl1/41 (gene therapy group C, GTC) injected TA at 23 weeks after injection (six mice). Developmentally regulated exons (filled boxes) are either dysregulated in DM (Clcn1, Ldb3/Cypher, Serca1, and Tnnt3) or not affected by the DM expansion mutations (Capzb and Itgb1). Primer positions (arrows) are illustrated below each autoradiograph within constitutively spliced exons (open boxes). The overexpressed mycMbnl1/41 is detectable only in the GTC mice (*Bottom*). Reprinted from *Reversal of RNA missplicing and myotonia after muscleblind overexpression in a mouse poly(CUG) model for myotonic dystrophy*; Kanadia RN, Shin J, Yuan Y, Beattie SG, Wheeler TM, Thornton CA, Swanson MS; Copyright 2006 Proc Natl Acad Sci U S A.

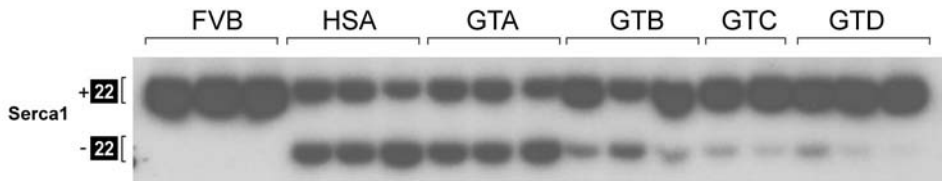


Figure 1-8. Time course for reversal of RNA missplicing. Complete recovery of myotonia at 23 weeks post- injection shows a robust reversal of missplicing. RT-PCR splicing assays of uninjected FVB/n and *HSA*$^{LR}$ (three mice each) or AAV2/1-mycMbnl1/41 (GTA, GTB, GTC and GTD) injected TA at 4, 12, 23 and 43 weeks after injection respectively (2 mice for GTC and 3 mice for other groups. For more results GTC group, see Figure 1-5). Developmentally regulated exon 22 of Serca1 (filled box) is dysregulated in DM.

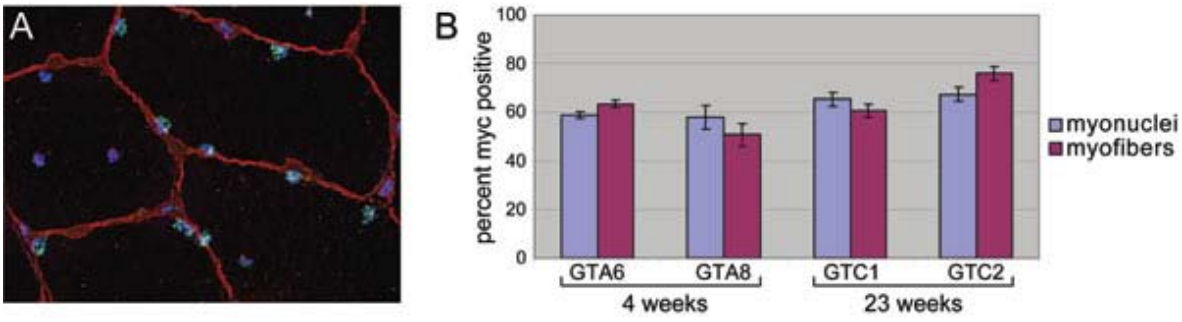


Figure 1-9. Ectopic mycMbnl1/41 expression after AAV2/1-mycMbnl1/41 injection. (*A*) Myonuclei expressing myc-tagged Mbnl1 were detected by using the anti-myc monoclonal antibody 9E10 (green), whereas myofibers were visualized by using TRITC-labeled wheat germ agglutinin (red), and nuclei were stained with DAPI (blue). (*B*) Quantification of myc-positive myonuclei and myofibers. The percentage of myonuclei expressing mycMbnl1/41 was determined by counting myc-positive and myc-negative nuclei in a representative region of each muscle (n = 2) for the 4-week (GTA6 and GTA8) and 23-week (GTC1 and GTC2) postinjection time points. Myonuclei were distinguished from interstitial nuclei by their location inside fibers rather than between fibers. Both subsarcolemmal and centrally located myonuclei were quantitated (blue). The percentage of myofibers that contained at least one myc-positive nucleus also was determined (purple). Reprinted from *Reversal of RNA missplicing and myotonia after muscleblind overexpression in a mouse poly(CUG) model for myotonic dystrophy*; Kanadia RN, Shin J, Yuan Y, Beattie SG, Wheeler TM, Thornton CA, Swanson MS; Copyright 2006 Proc Natl Acad Sci U S A.

# CHAPTER 2
# GENETIC FACTORS AFFECT DISEASE-ASSOCIATED PHENOTYPES IN MBNL1 KNOCKOUT MOUSE MODEL FOR MYOTONIC DYSTROPHY

## Introduction

### Myotonic Dystrophy is a Variable Disease

One of the remarkable characteristics of DM is the variability of disease phenotypes among patients. Symptoms vary greatly not only in severity (expressivity) but also in the percentage of patients who show the mutant phenotype (penetrance) (1). Not everyone displays all the disease-associated phenotypes and different patients are affected differently. Age-of-onset is also variable among patients even within the same family and some people are only affected mildly in later life whereas others develop problems much earlier. Generally, the number of CTG repeats has a positive correlation with the severity of disease. However, genetic and environmental variations also play important roles in disease penetrance (1, 2, 60).

Myotonia and muscle weakness/wasting are the two major muscle symptoms that occur in DM and it is muscle wasting that is the more troublesome for patients (61). Even though muscle is prominently affected, DM is not just a muscle disease. DM also affects other parts of the body and clinical manifestations include cardiac conduction defects and arrhythmia, bowel disturbances, balding in males and hypersomnolence (excessive daytime sleepiness). Less recognized disease-associated phenotypes include hormone problems, calcifying epithelioma and a higher incidence of cancer even though the association of DM with cancer is still a subject of debate (62-65).

Even with the significant progress in recent years, our knowledge is very limited in the understanding of the molecular defects underlying each one of these symptoms except for the example of myotonia and missplicing of *CLCN1*. Most of the studies so far have focused on elucidating common pathogenesis mechanisms for the disease. However, it is just as intriguing to ask why the symptoms of the disease are so variable and what is the molecular defect underlying such variability? In this study we will demonstrate that genetic factors play an important role in phenotypic variability of DM using a mouse model. We will also make an attempt to uncover molecular defects underlying DM-associated phenotypes by correlating the severity of certain phenotypes to a specific missplicing event.

**Mouse Models to Understand the Pathogenesis of DM**

Mouse models have been valuable tools to understand the molecular mechanisms of inherited diseases. A few mouse models have been generated to study DM including the *HSA*$^{LR}$ mouse discussed in Chapter 1 (17). *HSA*$^{LR}$ is a great model to prove that CTG expansions are toxic independent of gene context but it has limitations. First, the expression of CTG repeats is controlled by the human skeletal actin (*HSA*) promoter therefore *HSA*$^{LR}$ mice cannot model other non-skeletal muscle symptoms. Second, the number of repeats is only 250 and it does not recapitulate the whole spectrum of phenotypes observed for larger repeats. To overcome these limitations, additional transgenic mouse models have been developed. One is a human *DMPK* transgenic mouse which carries a larger CTG repeat (>300) in the DMPK 3' UTR (66-68). This mouse models the intergenerational repeat expansion (repeats tend to get larger in successive generations) that leads to the more severe form of disease. Histological abnormalities are seen in DMXL (CTG repeats longer

than 700) homozygous mice and severe body size retardation in DMXL/DMXXL mice (homozygous mice carrying 700 CTGs on one allele and >900 CTGs on the other allele) (66, 67). Aberrant splicing of target pre-mRNAs of DM such as Clcn1 is mild probably due to the low expression of transgene.

A more recently developed model is a tamoxifen inducible (interrupted) transgenic 960 CTG repeat mouse. The transgene contains a ubiquitously expressed CMV promoter, a floxed concatamer of the SV40 polyadenylation site, and human *DMPK* exon 15 containing 960 CTG repeats. When CTG repeats were induced in cardiac tissues by crossing with the MerCreMer (MCM) transgenic line, which expresses a heart-specific tamoxifen inducible Cre, bi-transgenic mice developed severe cardiac conduction defects as well as cardiomyopathy and died within 2 weeks (69). When 960 CTG expression was induced in skeletal muscle by crossing with HSA-Cre-ER$^{T2}$ line, in 4 weeks after tamoxifen administration these mice not only developed myotonia and muscle histopathology but also muscle wasting, which is a muscle phenotype that was absent in other DM mouse models (70). This result indicates that repeat number together with expression level are two important parameters for the muscle wasting phenotype.

Whereas the transgenic mice mentioned above demonstrate a fundamental role of CTG repeats in DM toxicity, other mouse models are employed to ask more direct questions pertaining to the molecular mechanism of DM. Based on the toxic RNA gain-of-function model, the roles of two splicing factors that are affected in DM have been evaluated using mouse models. Steady-state levels of Cugbp1 are upregulated in multiple DM tissues due to the phosphorylation of this protein via PKC kinase, and overexpression

of CUGBP1 in mouse results in the missplicing of subset of pre-mRNAs that are affected in DM (24, 34). These mice die around P8 and the shortened life span prevents investigation of the presence of other disease-associated phenotypes. In addition to increased CUGBP1 activity, MBNL1 function is compromised in DM due to sequestration. Since MBNL1 isoforms initiating from exon 3 have two pairs of C3H motifs that are required for RNA binding, the *Mbnl1* knockout (*Mbnl1*$^{\Delta E3/\Delta E3}$) mouse, in which exon 3 is deleted, is functionally null (Fig. 2-1). This mouse develops key clinical manifestations including myotonia, histopathology, cataracts and cardiac conduction defects (19).

Interestingly, phenotypes of *Mbnl1* knockout mice are variable in severity and penetrance. First of all, half of *Mbnl1*$^{\Delta E3/\Delta E3}$ mice die between 6-12 months of age whereas ~50% live a normal life span (~2 years). Attempts to determine the direct cause of death have been unsuccessful. Second, there is a penetrance issue for some disease-associated phenotypes. Myotonia and muscle pathology are present in every mouse that was tested, however, cardiac conduction defects (1$^{st}$ degree AV block) are present in only ~50% of mice tested at 8 weeks of age using telemetric electrocardiography (ECG). Aberrant splicing of a subset of pre-mRNAs affected in DM, such as Clcn1 and Tnnt3, is robust in every mouse tested. Physiological analysis for compromised muscle function has not been tested in these mice. Muscle wasting has not been observed, however, sudden death in ~50% of *Mbnl1*$^{\Delta E3/\Delta E3}$ mice prevented further investigation of the wasting phenotype. The *Mbnl1* knockout mouse is a good model for DM pathogenesis because it recapitulates most of the key features of disease but also models the incomplete penetrance of the disease.

**Influence of Genetic Background on Disease-Associated Phenotypes in Genetically Engineered Mice**

A number of studies have investigated the influence of genetic background on penetrance and expressivity in genetically engineered mice. (71). Differences between C57BL/6 (Bl6) and 129/Sv (129) genetic backgrounds are particularly interesting because null mutations in mice are usually generated with embryonic stem cells derived from 129 inbred strains and the resulting chimeric males are mated with Bl6 females which results in a mixed genetic background (72). Each strain has unique characteristics. For example, 129 mice have a high-anxiety phenotype with learning deficiencies and a high prevalence of developing gonadal teratomas (73, 74) while Bl6 mice often show low bone density, ocular defects and ulcerative dermatitis (75-77).

Generation of congenic strains for a mutant allele may lead to more consistent, or reveal additional, phenotypes. For example, caspase-3 deficient 129 mice are uniformly and severely affected by perinatal death and marked exencephaly whereas caspase-3 deficient Bl6 mice reach adulthood and show minimal brain pathology (78). Phenotypes of *Hdh* Q111 knock-in mice, which are a model for Huntington's disease (HD), show different intergenerational instability of the HD CAG repeat (CAG encodes glutamine) and intranuclear polyQ inclusion formation in Bl6 and 129 backgrounds (79).

Congenic lines also are valuable genetic tools to identify genetic modifiers that are responsible for the variability between strains. Genetic modifiers, which are genes that modify the effect produced by another gene (e.g. null allele in knockout mouse), are genetic variants that affect disease penetrance. For example, a single nucleotide polymorphism (SNP) of the MBL gene was identified as an important modifier in cystic fibrosis (CF). CF

patients carrying certain MBL alleles have a significantly less severe pulmonary phenotype, which suggests that the modifier locus could be a target for therapeutic intervention (80, 81). No significant genetic modifier has been identified for DM whereas animal studies suggest that transcription factor *Nkx2.5* may play role in modulating the severity of the cardiac phenotype in DM (82).

**Congenic *Mbnl1*$^{\Delta E3/\Delta E3}$ Mice and the Role of Mbnl1 in DM Pathogenesis**

As stated earlier, DM is a remarkably variable disease and both somatic mosaicism and genetic factors contribute to variability among DM patients. Since *Mbnl1*$^{\Delta E3/\Delta E3}$ mice faithfully recapitulate DM-associated phenotypes with incomplete penetrance for certain phenotypes such as cardiac conduction defects, we hypothesized that genetic background plays an important role in the clinical presentation of DM. In this study, we generated congenic *Mbnl1*$^{\Delta E3/\Delta E3}$ mice to ask several questions. Do different genetic backgrounds affect DM disease severity and penetrance? What is the consequence of loss of Mbnl1 protein on highly penetrant phenotypes such as myotonia and myopathy? What is the role of Mbnl1 in the development of non-muscle cells? We addressed these questions by characterizing Bl6 and 129 congenic mouse lines since this approach should enable us to understand the fundamental roles of Mbnl1 in DM pathogenesis as well as in the normal developmental process. We report that genetic background has a profound effect on the presentation of key disease features in *Mbnl1*$^{\Delta E3/\Delta E3}$ mice such as muscle weakness. Furthermore, we correlated muscle weakness with altered alternative splicing of specific genes that are important for calcium homeostasis, such as ryanodine receptor 1 (Ryr1). Our results support the possibility that muscle weakness in DM is not secondary to myotonia

and caused by a separate molecular defect. Finally, congenic mice developed in this study will be invaluable tools to identify genetic modifiers of DM disease.

## Results

### Effect of Genetic Background on Survival of *Mbnl1* Knockout Mice

To uncover disease-associated phenotypes that were masked in the original *Mbnl1*$^{\Delta E3/\Delta E3}$ mixed background, we generated congenic lines using a conventional backcross breeding strategy with either C57BL/6 (Bl6) or 129/Sv (129) inbred mice.

After ten generations of backcrosses, we analyzed the genotype ratio of pups at weaning age (~3 weeks) from heterozygous intercrosses for both genetic backgrounds by PCR analysis (Table 2-1). The genotype ratio for Bl6 mice was significantly skewed with a chi-square value of 32.67 ($p<0.005$). Only ~50% of *Mbnl1*$^{\Delta E3/\Delta E3}$ homozygous Bl6 mutants survived to weaning suggesting that Mbnl1 plays important roles during embryogenesis and/or the perinatal period. Mbnl1 is expressed at a moderate to high level in multiple embryonic tissues (31). In contrast, 129 mice showed a normal Mendelian ratio of 1:2:1 (WT:het:hom). The absence of Mbnl1 protein in both of Bl6 and 129 homozygous muscle tissues was confirmed by western blotting using the polyclonal anti-Mbnl1 antibody A2764 which confirmed PCR genotyping (Fig. 2-2 *A*).

### *Mbnl1*$^{\Delta E3/\Delta E3}$ 129 Mice Have Defects in Thymus and Skin Epithelium

We next examined morphological and histological properties of adult *Mbnl1*$^{\Delta E3/\Delta E3}$ congenic mice. The *Mbnl1*$^{\Delta E3/\Delta E3}$ mice backcrossed onto the 129 background developed normally during first 3 months of age. After this period, they displayed a high incidence of

sudden death and the survival rate of these mice decreased dramatically between 3-7 months of age. No *Mbnl1*$^{\Delta E3/\Delta E3}$ 129 mutant mice survived more than one year (Fig. 2-2 *B*).

A possible cause of the high mortality rate was a massive enlargement of thymus which occupied the entire thoracic cavity and compressed both the heart and lungs of *Mbnl1*$^{\Delta E3/\Delta E3}$ 129 mice. The mutant thymus was about 10 times larger (measured by wet weight) compared to that from wild type littermates at 24 weeks of age. Thymic enlargement was observed as early as 12 weeks of age and coincided with the onset of normal thymic involution in mice. Histological analysis revealed thymic hyperplasia demonstrating expansion of T lymphocytes (Fig 2-3 *A*).

Thymic T cell development involves distinct differentiation stages to provide a diverse T cell repertoire to fight against external invasion and induce tolerance to self antigens which involves the major histocompatibility complex (MHC) (83, 84). Double negative (DN) (CD4-CD8-) progenitors entering the thymic cortex from the bone marrow become DP (CD4+CD8+) cells following a pre-T-cell receptor (TCR) mediated selection signal. Mature SP thymocytes (CD4+CD8- or CD4-CD8+) that are released from the thymus then migrate to peripheral tissues. About 98% of thymocytes die during these developmental processes either by failing the positive or negative selection process. Preliminary studies on thymocytes from *Mbnl1*$^{\Delta E3/\Delta E3}$ 129 thymus indicated a dysregulation of the T-cell maturation process (Fig 2-3 *B*). Flow cytometry of thymocytes from *Mbnl1*$^{\Delta E3/\Delta E3}$ 129 mice showed that most T cells were stalled at the CD4+CD8+ DP stage whereas thymocytes from WT 129 mice showed a normal thymocyte distribution. Accumulation of DP T lymphocytes in *Mbnl1*$^{\Delta E3/\Delta E3}$ 129 mice is possibly due to the failure

of one of the selection steps, most likely negative selection, which deletes the majority of positively-selected T cells by reaction with self-antigen and apoptosis. In support of this hypothesis, in a preliminary study using anti-nuclear antibodies (ANA) test on human epidermoid cancer (HEp2)cell, *Mbnl1*$^{\Delta E3/\Delta E3}$ serum was positive for auto-antibodies even though we failed to identify the responsible antigen (data not shown).

*Mbnl1*$^{\Delta E3/\Delta E3}$ 129 mice also developed visible skin lesions around the eye lid, muzzle, dorsal neck and back. These lesions were generally dry and non-pruritic however they became progressively worse to the point that the affected mouse had to be sacrificed. Histological analysis revealed acanthosis, or hyperplasia of the epidermis, and severe inflammation of the dermal layer (Fig. 2-3 *C*).

### *Mbnl1*$^{\Delta E3/\Delta E3}$ Bl6 Mice Develop a Severe Movement Deficit and Muscle Abnormalities

Backcrossed *Mbnl1*$^{\Delta E3/\Delta E3}$ Bl6 mice were spared both thymic hyperplasia and dermatitis. Instead, *Mbnl1*$^{\Delta E3/\Delta E3}$ mice developed severe movement deficits and impaired motor coordination as early as 2 months of age. These mutants were easily distinguishable from their WT littermates by stiff extension hindlimb postures when the mouse was dropped from an ~20 cm height and movement slow with gait abnormalities characterized by a wobbling walk (Fig. 2-4 *A*). Muscle weakness and abnormal motor coordination were quantified by the rotarod assay (Fig. 2-4 *B*). During the four day training period, *Mbnl1*$^{\Delta E3/\Delta E3}$ 129 mice performed as well as WT littermates and were able to remain on the rotating/accelerating rod up to 2 min whereas *Mbnl1*$^{\Delta E3/\Delta E3}$ Bl6 mice with latency to fall of ~30 sec.

We analyzed the degree of electrical myotonia in multiple skeletal muscles (quadriceps, gastrocnemius, tibialis anterior) from Bl6 and 129 mutant mice because the movement deficit of *Mbnl1*$^{\Delta E3/\Delta E3}$ Bl6 mice was similar to that of the myotonic *Adr* mouse, which does not express any Clcn1 chloride channel(85). Electrical myography (EMG) was performed by inserting a needle electrode and recording the membrane potential of the stimulated muscle (Fig. 2-4 *C*). Surprisingly, 6 month old *Mbnl1*$^{\Delta E3/\Delta E3}$ Bl6 and 129 mice exhibited similar degree of myotonia in hindlimb (quadriceps, tibialis anterior, gastrocnemius) muscles while WT controls showed no electrical myotonia (n=4-6 for each genotype). Myotonia in myotonic dystrophy is caused by aberrant splicing of the major skeletal muscle chloride channel (Clcn1) that retains fetal exon 7a in adult muscles (39). Clcn1 splicing patterns in Bl6 and 129 mutant mice were also comparable with an equal ratio of exon 7a inclusion/exclusion, as expected from the EMG results, suggesting that myotonia is not the cause of the *Mbnl1*$^{\Delta E3/\Delta E3}$ Bl6 movement deficit (Fig. 2-4 *D*).

Histological examination of muscle from Bl6 mutant mice at 6 months of age showed distinct myopathic changes including centralized nuclei, split fibers and fiber size heterogeneity (Fig. 2-5 *A upper*) as reported in a previous study using *Mbnl1*$^{\Delta E3/\Delta E3}$ mixed background muscle (19). In contrast, 129 muscles showed only very mild changes and the percentage of *Mbnl1*$^{\Delta E3/\Delta E3}$ 129 myofibers with centralized nuclei was significantly lower than that of Bl6 mutants (5% and 16%, respectively) (Fig. 2-5 *C*).

Unlike human, mouse skeletal muscles, such as quadriceps and TA, are mostly composed of type II fast twitch fibers while other muscles such as soleus are ~70% type I slow twitch fibers (86). Type II muscles have two distinct classes. Type IIa fibers are more

oxidative with high mitochondrial content and are relatively slower in contractile properties compared to type IIb fibers which are more glycolytic (87). Immunofluorescence analysis of myosin heavy chain (MHC) isoforms revealed a change toward a more oxidative MHC with a large increase in type IIa fibers in Bl6 mutant quadriceps muscles (Fig. 2-5 *A lower*). A similar shift toward a more oxidative muscle phenotype was also observed for TA. Mitochondrial protein content is enriched in slower twitch oxidative fibers and this was detected by western blotting (Fig. 2-5 *B*). We observed an increase in cytochrome oxidase Va (Cox Va) level, which is a nuclear encoded protein that resides in the inner membrane of mitochondria, (88) by 3-fold in the Bl6 mutant compared with normal quadriceps muscle at 6 months of age. In contrast, Cox Va content in 129 mutant muscle lysate did not differ from WT controls. The increase in mitochondrial protein level is consistent with our observation of a shift toward type IIa fibers for Bl6 mutant muscles.

### Age Dependent Progression of Myopathic Changes and Aberrant Endplate Topology in *Mbnl1*$^{\Delta E3/\Delta E3}$ Bl6 Muscles

The morphological abnormalities observed at 6 months of age in the Bl6 mutant progressed with aging, and 15 month old mice exhibited more prominent changes and the presence of necrotic fibers as well as nuclear clumps, a sign of atrophy (Fig. 2-6 *left*). The percentage of myofibers with centralized nuclei increased up to ~50%. However, we did not observe any difference in muscle wet weight for the Bl6 mutant compared to WT, suggesting no obvious sign of wasting by 15 months.

In a mouse model for muscular dystrophy, chronic muscle damage often leads to the degeneration of neuromuscular junction (NMJ) (89). We analyzed the structure of the neuromuscular junction of 15 month old *Mbnl1*$^{\Delta E3/\Delta E3}$ Bl6 and WT muscles by labeling

acetylcholine receptors (AchR) with α-bungarotoxin (Fig. 2-6 *right*). TA muscles from WT Bl6 mice had a pattern of AChR staining that was smooth, continuous with extensive arborization. In contrast, ~80% of NMJs from Bl6 mutant muscle displayed a fragmented pattern of AChR staining characterized by discontinuous nerve ends, although small populations of intact NMJs were present with a normal continuous pattern of the AChR. We also analyzed the architecture of pre-synaptic axons and termini with antibodies against neurofilament and synaptic vesicles. In WT mice, axonal branches innervated well-defined post-synaptic structures showing complete overlap of pre- and post- synapses. In mutant mice, however, we observed incomplete overlap as well as axonal swelling indicating progressive denervation.

**Abnormal Contractile Properties in *Mbnl1*$^{\Delta E3/\Delta E3}$ Bl6 Muscles**

To investigate the physiological relevance of the dystrophic structural changes in *Mbnl1*$^{\Delta E3/\Delta E3}$ Bl6 muscles, we next evaluated muscle contractile properties of *Mbnl1*$^{\Delta E3/\Delta E3}$ Bl6 and 129 mice as well as WT controls. Our speculation was that the dystrophic histopathology correlates with muscle function and deficits in contractile properties would be seen in *Mbnl1*$^{\Delta E3/\Delta E3}$ Bl6 mice but not in 129 mutants. We isolated intact soleus and extensor digitorum longus (EDL) muscles from 3 month old mice and measured force generation of those muscle groups upon electric stimulation because they well represent slow type I muscle fibers and fast type II fibers, respectively. For soleus muscle (see Fig. 2-7), twitch force produced by direct stimulation with 1-ms current pulses did not show a significant difference between genotypes. However, in response to tetanic stimulation at 100Hz, *Mbnl1*$^{\Delta E3/\Delta E3}$ Bl6 muscles generated 21% less force compared to WT controls

whereas *Mbnl1*$^{\Delta E3/\Delta E3}$ 129 muscles contracted 20% more forcefully than their control counterparts. Due to an increase of muscle mass in *Mbnl1*$^{\Delta E3/\Delta E3}$ mice (19% for B6, $p=0.055$ and 28% for 129, $p<0.01$) when calibrated to the unit cross-sectional area (specific force), force from *Mbnl1*$^{\Delta E3/\Delta E3}$ Bl6 soleus muscle was 34% less than WT control while specific force of *Mbnl1*$^{\Delta E3/\Delta E3}$ 129 and WT were equivalent. Furthermore, both rapidity of contraction (time to peak) and the time to half-relaxation (T1/2R) were significantly decreased in *Mbnl1*$^{\Delta E3/\Delta E3}$ Bl6 soleus muscles (no change for *Mbnl1*$^{\Delta E3/\Delta E3}$ 129 muscles).

EDL muscles showed similar force measurement results (Fig. 2-8). *Mbnl1*$^{\Delta E3/\Delta E3}$ Bl6 muscles showed reduced force production both for twitch (21%) and tetanus (23%) ($p=0.01$ and 0.008 respectively) whereas 129 mice showed no difference. Specific force was reduced 27% in *Mbnl1*$^{\Delta E3/\Delta E3}$ Bl6 compared to WT even though the p-value was not statistically significant ($p=0.07$).

These results indicated that Mbnl1 loss-of-function leads to abnormal muscle pathology as well as altered contractile properties in slow and fast muscles in the Bl6 genetic background whereas 129 background mice are spared from these deficits. In addition, these data suggest that the degree of electrical myotonia caused by aberrant splicing of *Clcn1* is separable from histological and physiological abnormalities of skeletal muscles and it is likely that there are additional molecular defects that underlie muscle weakness in DM.

**Aberrant Splicing of Ryr1 Correlates with Myopathic Changes**

Mbnl1 is a splicing factor and the splicing of specific pre-mRNAs is affected in *Mbnl1*$^{\Delta E3/\Delta E3}$ mice. In an attempt to elucidate molecular defects underlying myopathic

changes in B6 mutant muscles, we compared the alternative splicing of *Mbnl1*$^{\Delta E3/\Delta E3}$ in both Bl6 and 129 backgrounds for genes that are important for muscle structure and function (Fig. 2-9). We tested the alternative splicing of ~30 genes and found that most of the targets that were affected in *Mbnl1*$^{\Delta E3/\Delta E3}$ showed no difference between genetic backgrounds, including SR/endoplasmic reticulum $Ca^{2+}$ ATPase 1 (Serca1) and myotubularin-related protein 3 (Mtmr3). Only 3 alternative exons were found to be differentially spliced between *Mbnl1*$^{\Delta E3/\Delta E3}$ Bl6 and 129 including the fetal exon of fast twitch troponin T (Tnnt3) and two exons of the ryanodine receptor 1 (Ryr1). The most significant change was in the alternative splicing of Ryr1 exon 70. Alternative exon 70 was predominantly excluded in B6 *Mbnl1*$^{\Delta E3/\Delta E3}$ mRNA (<1% inclusion of exon 70) while 8% inclusion of the exon was observed in *Mbnl1*$^{\Delta E3/\Delta E3}$ 129 muscle. Interestingly, both Tnnt3 and Ryr1 proteins are important cellular factors which determine the kinetics of contraction and calcium homeostasis in muscle. Tnnt3 is the tropomyosin-binding subunit of troponin that confers calcium sensitivity to skeletal muscle ATPase activity and Ryr1 encodes the SR calcium channel which releases calcium to trigger contraction.

### Mbnl1 Binds to Ryr1 Exon 70 RNA *in Vitro* but Does Not Regulate Splicing of an Ryr1 Minigene in C2C12 Cells

We investigated the molecular mechanism of *Ryr1* exon 70 splicing more carefully because previous studies have shown a direct role of for the peptide sequence encoded by this exon in excitation-contraction coupling (90). Exon 70 encodes the regulatory domain of Ryr1 and its exclusion results in enhanced calcium efflux from the SR in cultured myotubes. While Tnnt3 pre-mRNA is a well-characterized binding target of the Mbnl1 protein, with the binding motif YGCY in intron 8 near the 3' splice site, it is not clear if

Ryr1 pre-mRNA is a direct binding target even though alternative splicing of Ryr1 is altered in DM patient muscle as well as *HSA*$^{LR}$ mice (28, 57).

We first asked whether Mbnl1 binds to Ryr1 RNA by performing a photocrosslinking assay in which 293T cells were transfected with protein expression plasmid encoding myc-tagged MBNL1. Whole cell lysates were photocrosslinked with a $^{32}$P radiolabeled 600 nucleotide (nt) Ryr1 RNA flanking exon 70, RNA-protein complexes were pulled down using the 9E10 anti-myc monoclonal antibody and then these complexes were resolved by SDS-PAGE. Autoradiography showed that RNA for the region encompassing exon 70 crosslinked to the MBNL1 protein. Concurrently, the Ryr1 minigene was transfected into C2C12 cells to assay whether Mbnl1 overexpression changes Ryr1 splicing. The splicing pattern of Ryr1 minigene was not altered suggesting the possibility that Mbnl1 may be regulate Ryr1 splicing indirectly and thus other splicing factors are responsible for the aberrant splicing of Ryr1 in B6 *Mbnl1*$^{\Delta E3/\Delta E3}$ mice.

## Discussion

*Mbnl1* is highly expressed in skeletal muscle, heart, brain and lymphoid organs, such as thymus and spleen, in the mouse (31). In a previous study, our lab showed that the loss of *Mbnl1* results in myotonia and histopathological anomalies in skeletal muscle (19). However, other disease-associated phenotypes, such as muscle wasting and cardiac conduction defects, were absent or less penetrant. Also the initial study lacked a thorough characterization of the mouse model and it was not clear as to what extent the loss of MBNL1 function has a role in DM pathogenesis. In this study, we generated congenic (either B6 or 129) *Mbnl1* knockout mice and our results provide evidence that two major

muscle phenotypes in DM, myotonia and muscle weakness, are separable events and that Mbnl1 may be responsible for the muscle weakness in DM possibly through altered alternative splicing of Ryr1 exon 70. Furthermore, we uncovered additional phenotypes such as the abnormal morphology of NMJs in *Mbnl1* knockout mice.

The most striking observation that we have made during the course of this study is that genetic background has a profound effect on the presentation of DM-associated phenotypes in these mice, which suggests that other genetic factors contribute to the variability of DM. The first noticeable difference between congenic mice in the two different backgrounds was the survival rate. For $Mbnl1^{\Delta E3/\Delta E3}$ Bl6 mice, a high level of lethality occurred (~50%) by 3 weeks of age. We have not investigated the cause of early lethality. However, it would be interesting to see if this population shows a retardation in embryonic muscle development, which can be seen in the congenital form of DM. Bl6 mice still have variability in the onset of lethality even after a 10 generation backcross possibly because they still carry a129 region flanking and including the *Mbnl1* null allele. It is possible that a genetic modifier that affects Mbnl1 function is linked to *Mbnl1* locus on chromosome 3, and the modifier allele plays a role in determining the life span of the mutant mice.

In contrast, 129 mice showed perfect 1:2:1 segregation ratio from heterozygous intercrosses and they were completely normal by 3 month of age until they developed phenotypes such as thymic hyperplasia and skin defects. Thymic enlargement occurs due to a large number of proliferating lymphocytes which are mostly CD4+ CD8+ DP cells. Other mouse models with DP T lymphocyte expansion include the *Ft* (*Fused toes*) mouse with

deletion of *IrxB* gene cluster caused by thymic stromal cell defects as well as acetylcholinesterase (AchE)-R variant overexpression transgenic mice that are implicated in myasthenia gravis (MG). The thymocytes from this latter mouse were more resistant to apoptosis suggesting a failure in selection (91-93).

It is not clear whether the accumulation of immature T lymphocytes is due to defective signaling from thymic epithelial cells or is a T cell autonomous problem. One possibility that explains immature T cells retained in the *Mbnl1*$^{\Delta E3/\Delta E3}$ thymus is disrupted regulation of cell migration and signaling pathways. For example, fibronectin (FN) is a multifunctional extracellular matrix glycoprotein, which plays a role not only in providing a scaffold for cells but also in cell migration and signaling to adhering cells (94). *Mbnl1*$^{\Delta E3/\Delta E3}$ mice have an aberrant inclusion of the extradomain EDA and EDB exons which are found in onco-fetal tissues. It is tempting to speculate that such a defect in splicing leads to altered cell migration or apoptosis that results in thymic enlargement in *Mbnl1*$^{\Delta E3/\Delta E3}$ mice. Also, it is not clear why only *Mbnl1*$^{\Delta E3/\Delta E3}$ 129 male mice develop this phenotype (>90% penetrant) while females develop skin lesions. One possibility is that dysregulation of a sex specific gene underlies the thymic phenotype. Indeed, castration of normal male rodents results in a significant enlargement of the thymus, and androgen replacement can rescue the defect. It has been suggested that the androgen receptor (AR) expressed by thymic epithelial cells is an important player in thymocyte development even though we failed to detect any obvious missplicing of the AR gene (95).

To identify molecular defects underlying thymic phenotypes of *Mbnl1*$^{\Delta E3/\Delta E3}$ mice, we have tested alternative splicing patterns of the TCRζ receptor as well as other key

factors that are known to regulate DP to SP differentiation, including Zap70, Id2, Cd3d, Cd45, Ptcra and transcription factor Aire. Hwoever, we failed to identify any significant changes in splicing. Regardless, involvement of Mbnl1 in T cell development is an interesting observation and worth further investigation since a fundamental role for other splicing factors, such as SC35 and HuR, in thymic T cell development has been observed (96, 97). Because Mbnl1 translocates to the nucleus during a specific developmental window (between P2 and P20 for skeletal muscle), it would be interesting to see if this translocation occurs during the same period in thymic T cells as well (33).

There is no evidence for defective T cell development in DM. However, several case reports exist which show the development of benign thymomas in DM patients. Thymomas originate from epithelial cell populations in the thymus (98-100). In addition, a subpopulation of DM patients is affected with pilomatrixomas, which is a benign tumor of the face, neck or proximal upper extremity, possibly due to altered epithelial cell function (63, 64). This observation supports the idea that epithelial cell changes may underlie the thymic and skin phenotypes in *Mbnl1*$^{\Delta E3/\Delta E3}$ 129 knockout mice. Generally, pilomatrixomas are associated with mutations in genes of the Wnt signaling pathway. However we failed to detect altered splicing of these genes although further studies will be required to confirm that the dermatitis in *Mbnl1*$^{\Delta E3/\Delta E3}$ 129 mice and pilomatrixomas in DM patients are similar (101). Also, there is a recent case report of a DM patient with basal and squamous cell carcinomas that are similar to the skin lesions noted in *Mbnl1*$^{\Delta E3/\Delta E3}$ 129 mice (65).

Muscle weakness is evaluated using a force measurement protocol. It is a commonly used method to evaluate muscle function in muscular dystrophy. In our study, we clearly

showed that *Mbnl1*$^{\Delta E3/\Delta E3}$ Bl6 mice have defective contractile properties, especially in specific force deficit. It was also striking that *Mbnl1*$^{\Delta E3/\Delta E3}$ 129 mice are spared muscle weakness at least until 3 months of age. It is possible that the 129 mice will develop weakness at later stage however the shortened life span prevented us from investigating this possibility. *Mbnl1*$^{\Delta E3/\Delta E3}$ Bl6 muscles were also enriched in oxidative fibers, which is indicated by an increase of type IIa MHC positive fibers and a high mitochondrial protein expression. It is well known that chronic stimulation can result in a fiber type switch toward more oxidative fibers (102). In this study we have shown that *Mbnl1*$^{\Delta E3/\Delta E3}$ Bl6 and 129 mice have equivalent degrees of myotonia not only by EMG but also by the Clcn1 splicing pattern, which suggests that myotonia is not the main cause of the abnormal structure nor muscle weakness in DM. This idea is supported by the observation that the myotonic *adr* mouse muscle has relatively minor histological changes except the absence of type IIb fibers (85, 103, 104). Our results provide the first direct evidence that Mbnl1 loss-of-function underlies muscle weakness by altering both structural and functional properties of skeletal muscles.

Another interesting observation is the progressive muscle pathology. By 15 months of age, myofibers with dystrophic changes increased up to 50% in quadriceps and TA. These changes were accompanied by abnormal NMJ structure. The morphological NMJ abnormalities appear to be degenerative rather than developmental since we did not observe a similar discontinuous pattern of AChR staining in the young (2 month old) *Mbnl1*$^{\Delta E3/\Delta E3}$ Bl6 TA muscles. It is not clear whether these NMJ changes result from motor neuron defects or are am product of skeletal muscle defects. However, intact NMJs are essential to

propagate action potentials from motor neurons. Therefore, aberrant endplate topology in Bl6 mutants suggests that the movement deficits seen in these mice might result from abnormal NMJ formation and physiological dysfunction of the NMJ.

Discontinuous junctions in skeletal muscles have been observed in other mouse models for muscular dystrophy such as the *mdx* mouse and *mdx/utrophin* double knockout mice and it was suggested that the absence of dystrophin leads to abnormal AChR-cytoskeleton interactions (89). Recently, there was a report that human *DMPK* transgenic mice with 300 or more CTG repeats exhibit abnormal NMJ in the diaphragm muscle. However, this study is the first to report an abnormal end plate morphology in skeletal muscle of a mouse model for DM (105). Significant fragmentation of the AChR in *Mbnl1*$^{\Delta E3/\Delta E3}$ muscle could lead to a reduction in the transmission of action potentials from motor neurons to muscles, which may explain muscle wasting in DM. As shown for other muscular dystrophies, muscle atrophy is related to motor neuron denervation. In support of this hypothesis, it has been demonstrated that the *DMPK* gene is expressed at high level in subsynaptic myonuclei in human skeletal muscles and toxic $(CUG)_n$ RNA and MBNL1 proteins are retained in postsynaptic nuclei in the NMJ region in DM muscle (106). Absence of a muscle wasting phenotype in *Mbnl1*$^{\Delta E3/\Delta E3}$ mice is possibly due to the high regeneration level observed in rodents. Similarly, in the *mdx* mouse, which is a model mouse for Duchenne muscular dystrophy, necrosis is compensated by active regeneration and these mice fail to develop muscle atrophy (107, 108). Alternately, the muscle wasting phenotype may result from the loss of function of another factor unrelated to MBNL1. The

observation that $(CUG)_{960}$ mice develop muscle wasting supports the possibility that large CUG repeats sequester other trans-activating factors resulting in a wasting phenotype.

Muscle weakness and structural defects in *Mbnl1*$^{\Delta E3/\Delta E3}$ Bl6 mice correlate with altered splicing of *Tnnt3* fetal exon, *Ryr1* exons 70 and 83. Mutations of *Ryr1* have already been linked to other skeletal myopathies such as central core disease, which causes hypotonia and proximal muscle weakness (109). Among two alternative exons of Ryr1, exon 70 exclusion in *Mbnl1*$^{\Delta E3/\Delta E3}$ B6 muscle is of particular interest because the aberrant splicing of this exon has been demonstrated in DM and *HSA*$^{LR}$ muscles (57). A previous study, Ryr1 peptides with or without exon 70 were expressed in dyspedic (*Ryr1* null) myotubes *in vitro* to test the functional readout of missplicing Calcium ($Ca^{2+}$) release was enhanced by >50% in myotubes without exon 70 compared to myotubes with exon 70 (90). Increased $Ca^{2+}$ release can result in myopathy if it leads to sustained rise in intracellular $Ca^{2+}$ in muscle. A profound alteration in $Ca^{2+}$ homeostasis can lead to a disruption in $Ca^{2+}$-mediated cell signaling. For example calpain, $Ca^{2+}$-dependent protease, activation can occur. Supporting this hypothesis, *Mbnl1*$^{\Delta E3/\Delta E3}$ Bl6 quadriceps muscle showed considerably higher calpain activity compared to WT ($p=0.065$) whereas 129 mice showed no changes (n=3, each genotype). This assay was not sensitive enough to distinguish between different types of calpains and it should be repeated with more samples and a more sensitive assay for specific calpain activities. Moreover direct measurement of $Ca^{2+}$ efflux from SR as well as $Ca^{2+}$ sensitivity of *Mbnl1*$^{\Delta E3/\Delta E3}$ muscle should be performed to demonstrate dysregulaiton of $Ca^{2+}$ homeostasis.

What is the molecular mechanism underlying the different regulation of Ryr1 alternative splicing in different genetic backgrounds? One possible model, which involves a genetic modifier that functions as a splicing factor, is presented in Fig. 2-10. Both MBNL1 and this splicing factor (X) interact with a spliceosome factor such as a component of U1 snRNP and stabilize the interaction of the pre-mRNA/spliceosome complex at the 5' splice site of Ryr1 exon 70. In the Bl6 background, splicing factor X is either absent or functionally compromised leading to decreased Ryr1 exon 70 inclusion (~80%) compared to 129 background (~90%). In *Mbnl1*$^{\Delta E3/\Delta E3}$ tissues, exon 70 is predominantly excluded due to loss of Mbnl1 function. The presence of the genetic modifier in the 129 background enhances the inclusion ratio to 9%, which might be result in the normal muscle structure and function of the *Mbnl1*$^{\Delta E3/\Delta E3}$ 129 mouse. However in *Mbnl1*$^{\Delta E3/\Delta E3}$ Bl6 tissues, inclusion of exon 70 is less than 1% due to the absence, or decreased activity, of the genetic modifier X.

What is a possible candidate for the genetic modifier X? The *Scnm1* locus is a trans-activating modifier that determines the severity of a sodium channelopathy in mice (110). Scnm1 is an auxiliary spliceosomal protein that contributes to the recognition of non-consensus 5' splice sites. The phenotype of the hypomorphic allele of *Scn8a* (medJ) is dependent upon the *Scnm1* locus (111-113). Bl6 carries a variant allele *Scnm1*$^{R187X}$ that results in a more severe phenotype compared to other strains because the C-terminal domain of Scnm1 is truncated in Bl6, and not in the other strains, and this leads to increased exclusion of exon 2 and 3 of *Scn8a* because this domain mediates the interaction with LUC7L2, which is a mammalian homolog of a yeast protein involved in recognition of

non-consensus splice sites. Interestingly, only a 5% difference in exon exclusion (10% correct transcripts in other strains and 5% in B6) is enough to yield a significant difference in neurological phenotype, which suggests that slight changes in splicing due to genetic modifiers have profound effects on disease severity.

It is an interesting idea to test whether Scnm1 is the genetic modifier X. Alternatively the genetic modifier X can be a different splicing factor or a novel locus. Since the expression of the modifier in 129 tissues was sufficient to repress the disease-associated phenotypes, such as centralized nuclei in myofibers as well as compromised force generation, it is important to identify the genetic modifier. This putative splicing factor is an interesting potential therapeutic target for muscle weakness in DM.

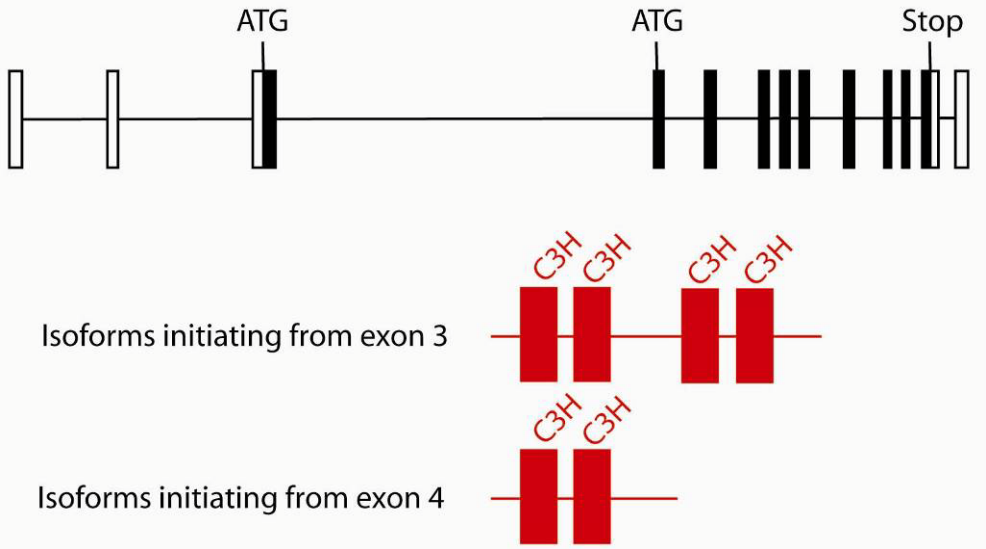


Figure 2-1. The *Mbnl1*$^{\Delta E3/\Delta E3}$ mouse is a functional null. Schematic representation of the *Mbnl1* gene (black line). Exons that encode UTRs (open boxes) and ORFs (black boxes) are indicated. Isoforms that initiate in exon 3 contain four copies of C3H (4XC3H) whereas the isoforms that use the exon 4 initiation codon contain only two C3H motifs (2XC3H). *Mbnl1*$^{\Delta E3/\Delta E3}$ mouse is a functional null since 4XC3H containing isoforms are missing.

| Strain | # of progeny | *Mbnl1* $^{+/+}$ | *Mbnl1* $^{+/\Delta E3}$ | *Mbnl1* $^{\Delta E3/\Delta E3}$ | Chi-square | p-value |
|---|---|---|---|---|---|---|
| | | | | | (1:2:1) | |
| Bl6 | (observed) | 130 | 193 | 52 | 32.67 | < 0.005 |
| | (expected) | 94 | 188 | 94 | | |
| 129 | (observed) | 112 | 209 | 95 | 1.398 | NS |
| | (expected) | 104 | 208 | 104 | | |

Table 2-1. Genotypic evaluation of B6 and 129 congenic mice. Pups from heterozygous intercrosses were genotyped at weaning age (~3 weeks). Comparison of observed and expected genotypic ratio is presented along with chi-square value and corresponding p-value. A significant percentage of *Mbnl1*B6 knockout mice showed embryonic to perinatal lethality.

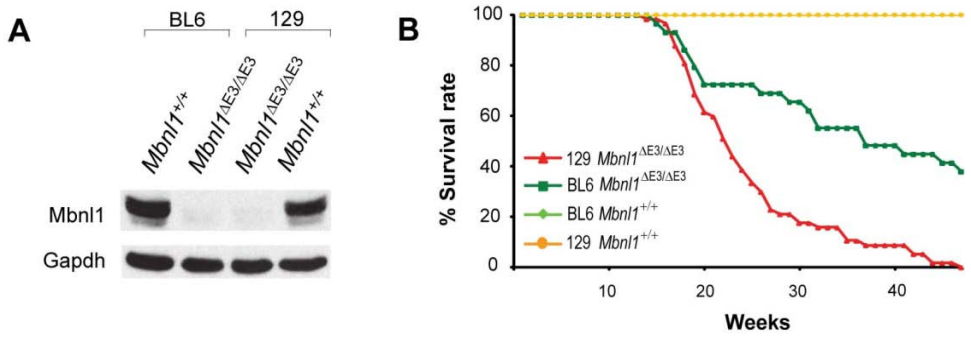


Figure 2-2. Shortened life span in congenic *Mbnl1*$^{\Delta E3/\Delta E3}$ Bl6 and 129 mice. (*A*) Mbnl1 protein is completely absent in quadriceps muscles of *Mbnl1*$^{\Delta E3/\Delta E3}$ mice in both backgrounds when total protein is blotted with anti-Mbnl1 polyclonal antibody. Gapdh is the protein loading control. (*B*) Kaplan-Meier survival curve is shown for *Mbnl1*$^{+/+}$ 129 (yellow), *Mbnl1*$^{\Delta E3/\Delta E3}$ 129(red), *Mbnl1*$^{+/+}$ Bl6 (light green) and *Mbnl1*$^{\Delta E3/\Delta E3}$ Bl6 green). Enhanced lethality of *Mbnl1*$^{\Delta E3/\Delta E3}$ Bl6 mice was seen between 12 weeks and 26 weeks of age whereas lethality of *Mbnl1*$^{\Delta E3/\Delta E3}$ Bl6 mice was gradual. 100% of WT mice survived for the same time period.

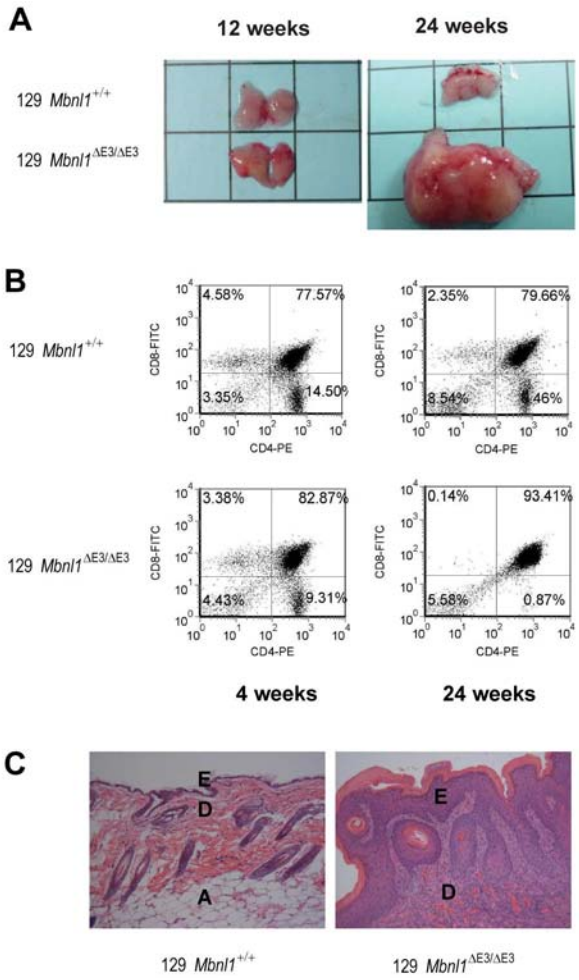


Figure 2-3. *Mbnl1*$^{\Delta E3/\Delta E3}$ 129 congenics have defects in thymus and skin. (*A*) Enlargement of the thymus in *Mbnl1*$^{\Delta E3/\Delta E3}$ 129 congenics at 24 weeks of age. The size of the thymus in mutant mice was comparable to WT at 12 weeks of age while there is massive enlargement of thymus at 24 weeks of age. Rectangle in the background is 1cm$^2$. (*B*) Enlargement of the thymus in 129 knockout mice at 24 weeks of age is correlated with expansion of immature T lymphocytes. Flow cytometry of thymocytes from *Mbnl1*$^{\Delta E3/\Delta E3}$ 129 mice show defects in differentiation of T cells from double positive (CD4+CD8+) to single positive (CD4+CD8- or CD4-CD8+) stage. Cells were gated for CD4+ positive and CD8+ positive population. (*C*) Histological analysis of 129 skin by H&E staining. E=epidermis, D=dermis, A=adipose. *Mbnl1*$^{\Delta E3/\Delta E3}$ 129 skin shows severe hyperplasia of epidermis as well as inflammation of the dermal layer. The thick keratinous layer above the epidermis is also noticeable.

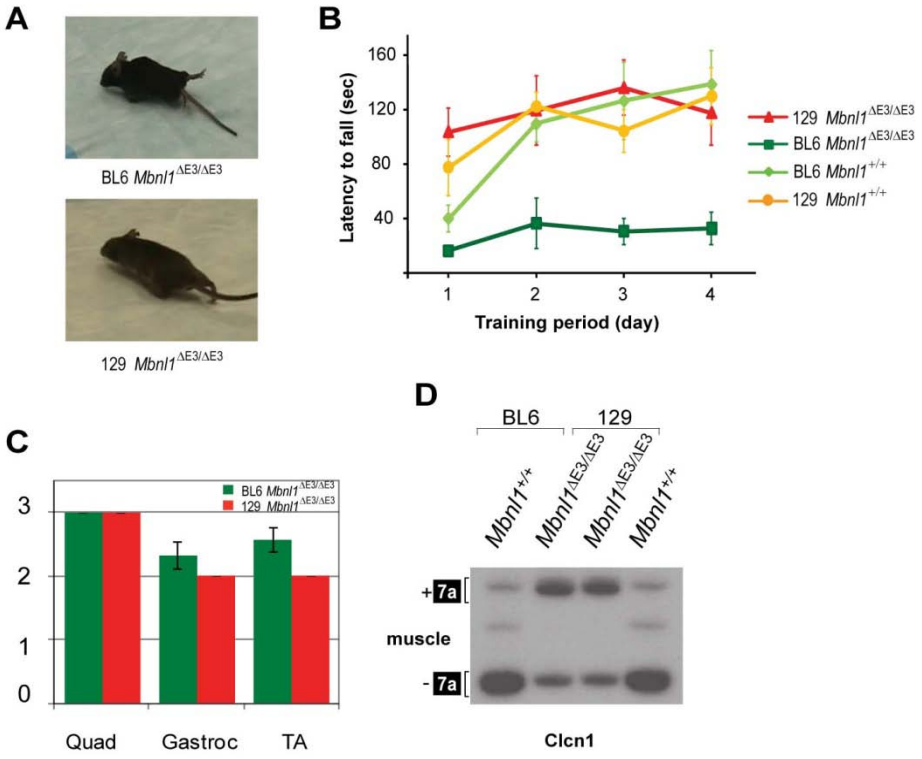


Figure 2-4. Severe movement deficit in B6 *Mbnl1*$^{\Delta E3/\Delta E3}$ mice is separable from myotonia. (*A*) *Mbnl1* Bl6 knockout mice developed severe movement deficits shown by stiff hindlimb postures. *Mbnl1* 129 knockout mice are much less affected. (*B*) Abnormal motor coordination of 3-4 month old *Mbnl1*$^{\Delta E3/\Delta E3}$ B6 mice measured by latency to fall using the accelerating rotarod. The rotarod starts at 4 rpm and accelerates to 40 rpm for first 2 min. The performance of *Mbnl1*$^{\Delta E3/\Delta E3}$ 129 mice was comparable to WT controls. Genotypes (color coded) are: *Mbnl1*$^{\Delta E3/\Delta E3}$ Bl6 (green), *Mbnl1*$^{+/+}$ Bl6 (light green), *Mbnl1*$^{\Delta E3/\Delta E3}$ 129 (red) and *Mbnl1*$^{+/+}$ 129 (yellow). (*C*) Myotonia was assessed by EMG on B6 (green) or *Mbnl1*$^{\Delta E3/\Delta E3}$ 129 mice (red) in the multiple skeletal muscle tissues. Difference in the degree of myotonia in the two groups is not significant. The EMG scale is: 0, no myotonia; 1, occasional myotonic discharge in <50% of needle insertions; 2, myotonic discharge with >50% of insertions; 3, myotonic discharge with nearly all insertions. WT mice for both genetic backgrounds were also tested and they were all 0. (*D*) RT-PCR splicing assay of congenic muscles for Clcn1 agreed with the EMG results. The ratio of alternative exon 7a inclusion was equivalent in *Mbnl1*$^{\Delta E3/\Delta E3}$ mice in both backgrounds. Alternative exon 7a (black box) is dysregulated in DM as well as DM mouse models.

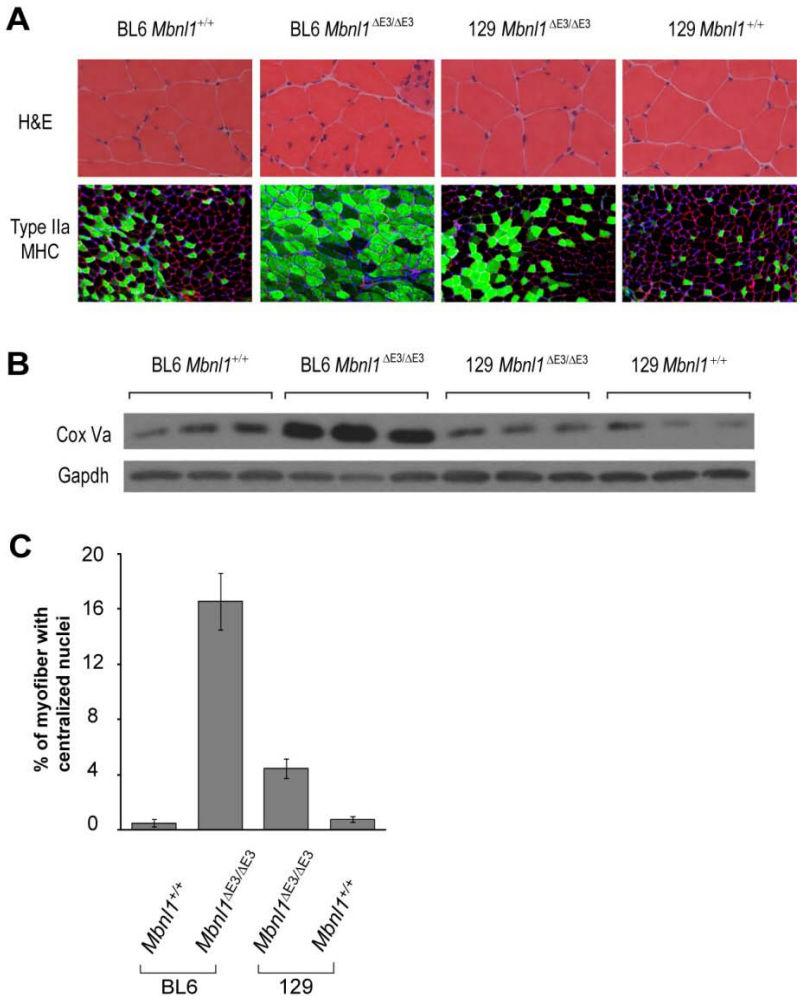


Figure 2-5. Abnormal muscle structure and fiber type switch in *Mbnl1*$^{\Delta E3/\Delta E3}$ Bl6 muscle. (*A*) Muscle histology (H&E staining) of quadriceps muscle sections from 6 month old Bl6 and 129 WT and mutants *Mbnl1*$^{\Delta E3/\Delta E3}$ Bl6 mice show abnormal muscle structures, such as centralized nuclei and split fibers, whereas *Mbnl1*$^{\Delta E3/\Delta E3}$ 129 muscles are much less affected. Immunohistochemistry of muscle sections with an antibody specific for type IIa MHC (green) shows muscle fiber type changes in *Mbnl1*$^{\Delta E3/\Delta E3}$ Bl6 toward more oxidative fiber type IIa. Muscle sections were costained with laminin anitibody (red) and DAPI (blue) to localize individual myofibers and nuclei. (*B*) *Mbnl1*$^{\Delta E3/\Delta E3}$ Bl6 muscles are enriched in mitochondrial protein. Total protein lysates of quadriceps muscles from Bl6 and 129 mice were probed with mitochondrial protein Cox Va specific antibody. Gapdh is a glycolytic protein and is slightly downregulated in *Mbnl1*$^{\Delta E3/\Delta E3}$ Bl6 muscles. (*C*) Percentage of myofibers with centralized nuclei is quantified from the muscles sections from (*A*). Average of >1400 fibers were counted for each genotype.

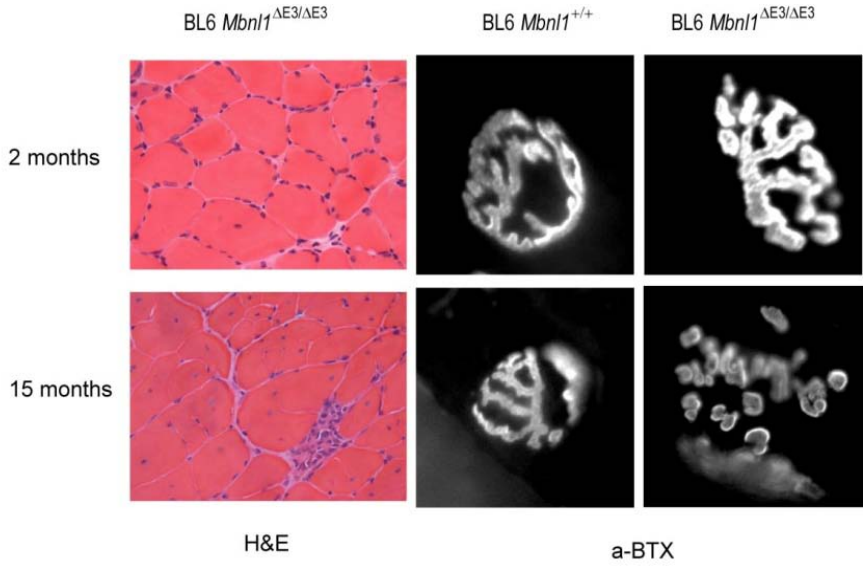


Figure 2-6. Age-dependent progressive muscle histopathology and abnormal end plate topology. (*Left*) H&E staining of TA muscles of *Mbnl1*$^{\Delta E3/\Delta E3}$ Bl6 mice at 2 months of age shows almost normal structure. Histopathological abnormalities such as centralized nuclei and split fibers progress with ageing. There is also very high heterogeneity in myofiber size. (*Right*) Structure of neuromuscular junctions (NMJs) in TA muscles was analyzed by labeling acetylcholine receptors (AchR) with α-bungarotoxin. At 2 months of age, the NMJ of *Mbnl1*$^{\Delta E3/\Delta E3}$ mouse had a smooth and continuous pattern of AChR staining whereas ~80% of NMJs of the 15 month old Bl6 mutant mouse showed a fragmented pattern of AChR staining characterized by discontinuous nerve ends, although a small population of intact NMJs was present. Wild type littermates showed normal NMJ structures at all time points.

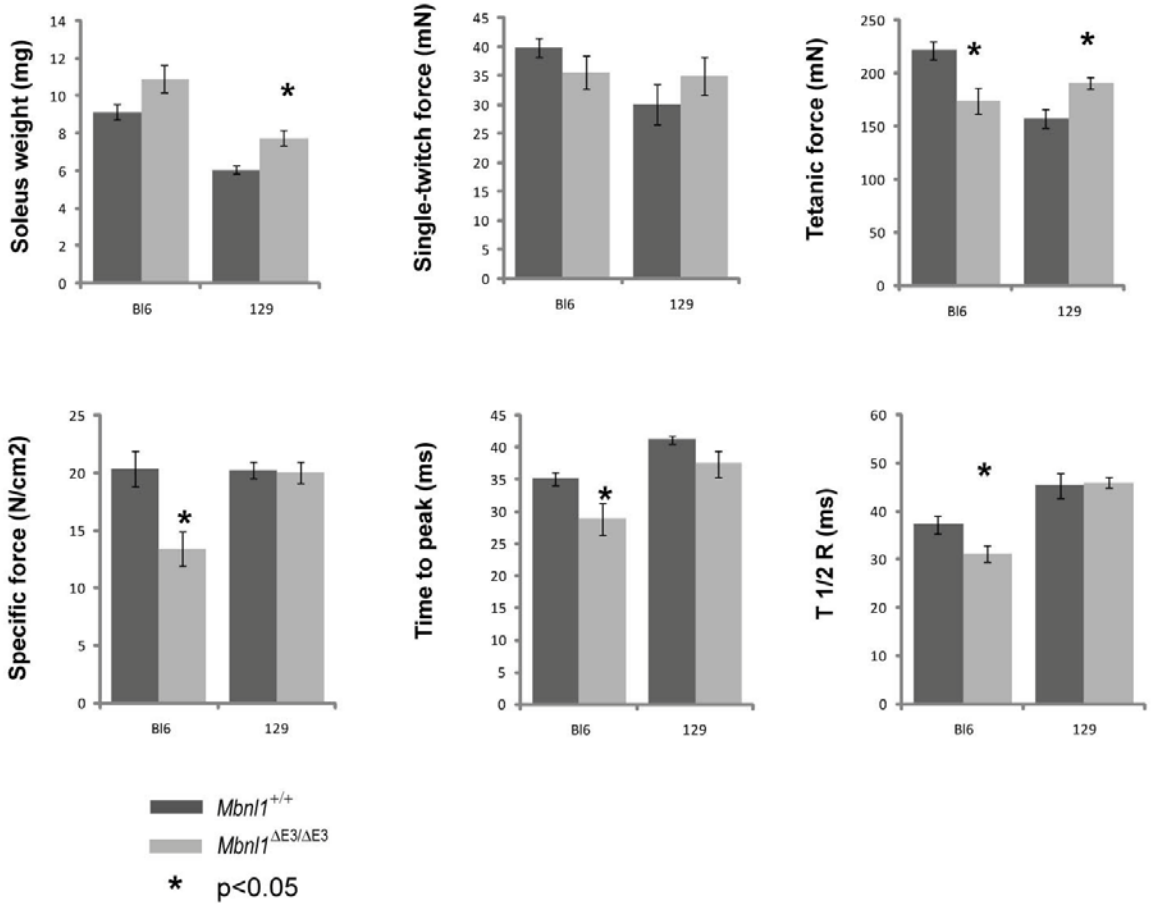


Figure 2-7. Reduced force and abnormal contraction-relaxation kinetics of *Mbnl1*$^{\Delta E3/\Delta E3}$ Bl6 soleus muscles. Three month old *Mbnl1*$^{+/+}$ (dark grey) and *Mbnl1*$^{\Delta E3/\Delta E3}$ (light grey) soleus muscles in Bl6 and 129 backgrounds were subjected to force measurements. Single twitch contraction produced by a 1ms current pulse did not show a significant difference whereas titanic stimulation at 100Hz produced 21% less force in *Mbnl1*$^{\Delta E3/\Delta E3}$ Bl6 soleus compared to WT controls. *Mbnl1*$^{\Delta E3/\Delta E3}$ 129 muscles showed 20% more titanic force than their control muscles. Due to the increase of muscle mass in *Mbnl1*$^{\Delta E3/\Delta E3}$ mice (19% for B6, $p=0.055$ and 28% for 129, $p<0.01$) when calibrated to the unit cross-sectional area (specific force), force from *Mbnl1*$^{\Delta E3/\Delta E3}$ Bl6 soleus muscle was 34% less than WT control while specific force of *Mbnl1*$^{\Delta E3/\Delta E3}$ 129 and WT was equivalent. Furthermore, time to peak and T1/2R decreased suggesting changes in kinetics in contraction and relaxation of *Mbnl1*$^{\Delta E3/\Delta E3}$ Bl6 soleus muscles.

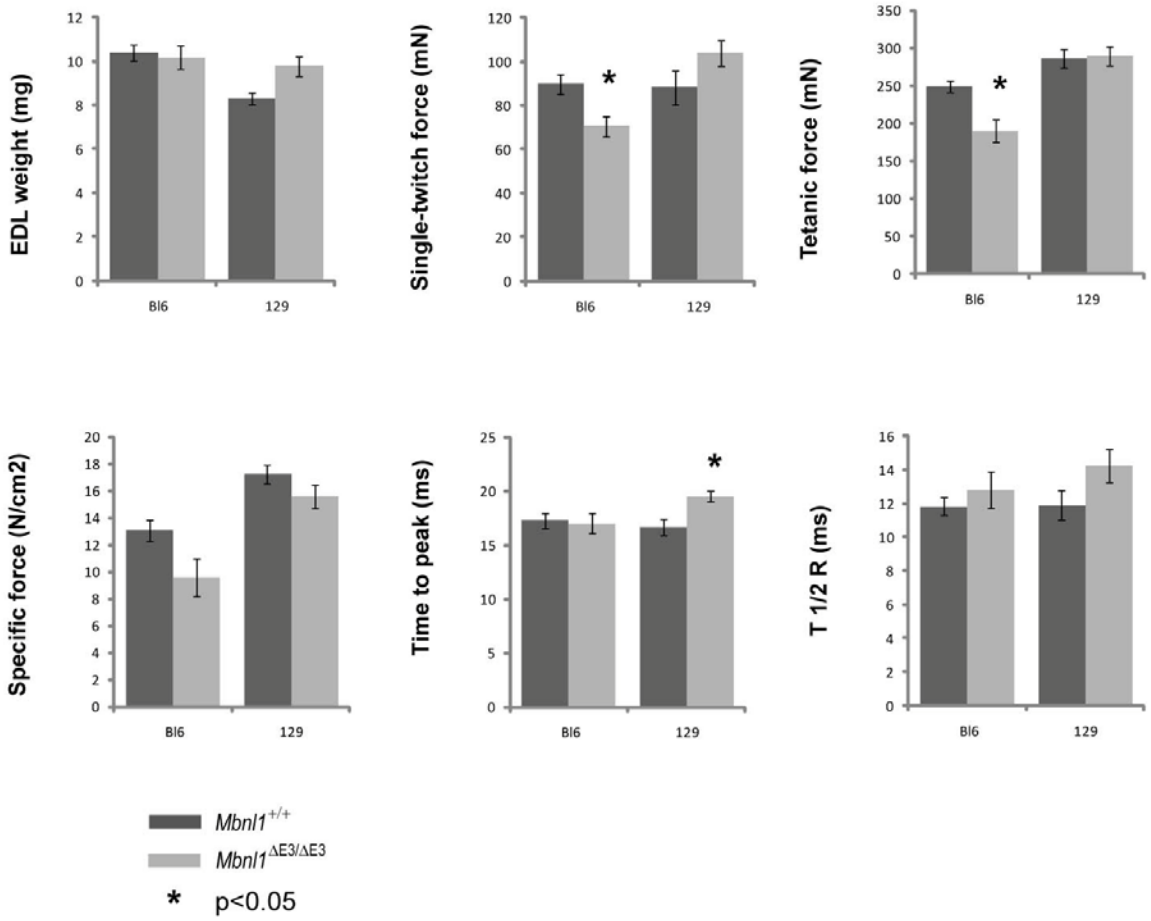


Figure 2-8. Reduced force generation of *Mbnl1*$^{\Delta E3/\Delta E3}$ Bl6 extensor digitorum longus (EDL) muscles. Three month old *Mbnl1*$^{+/+}$ (dark grey) and *Mbnl1*$^{-/-}$ (light grey) EDL muscles in B6 and 129 backgrounds were subjected to measure force production. Single twitch contraction produced by a 1ms current pulse generated 21% less force in *Mbnl1*$^{\Delta E3/\Delta E3}$ Bl6 EDL compared to WT controls (p=0.008). Titanic stimulation at 100Hz produced 23% less force in *Mbnl1*$^{\Delta E3/\Delta E3}$ Bl6 EDL compared to WT controls (p=0.01). *Mbnl1*$^{\Delta E3/\Delta E3}$ 129 muscles were identical to their WT controls. When calibrated to the unit cross-sectional area (specific force), force from *Mbnl1*$^{\Delta E3/\Delta E3}$ Bl6 EDL muscle was considerably (not significantly) lower than WT control (p=0.07).

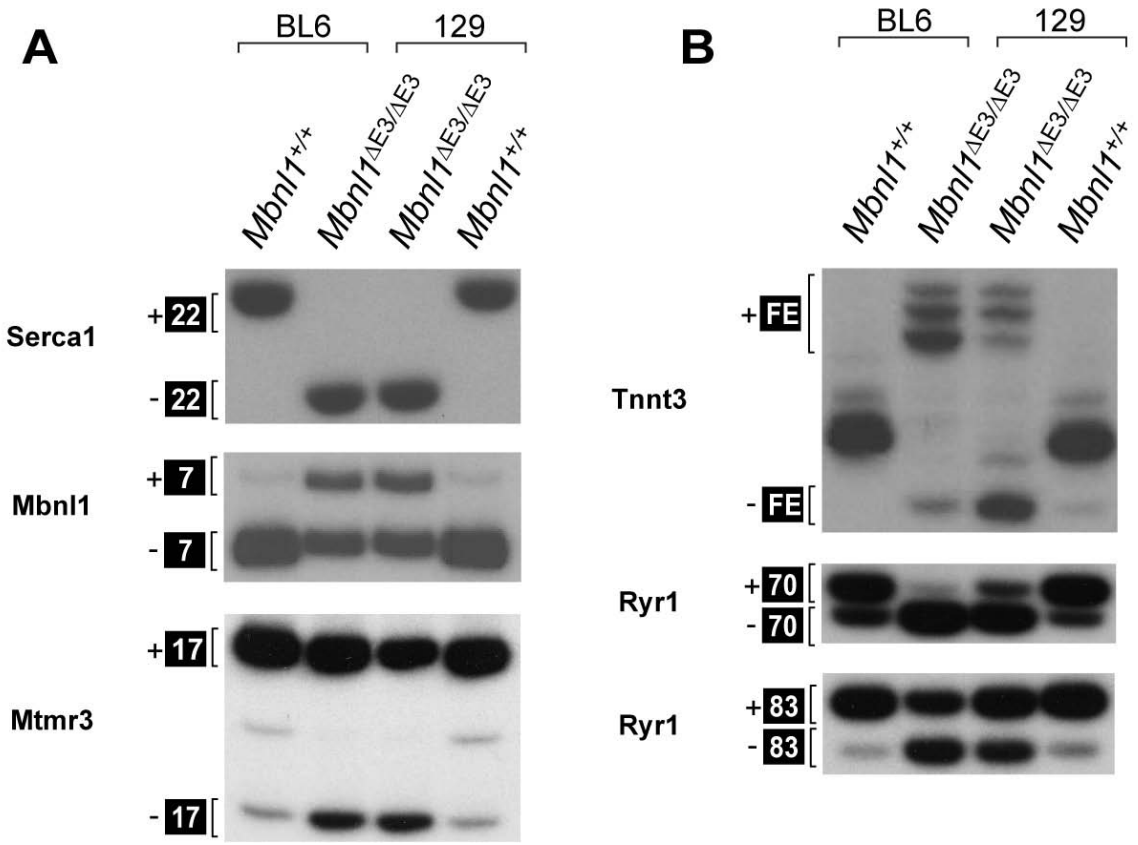


Figure 2-9. Aberrant splicing of Ryr1 and Tnnt3 are correlated with myopathic changes of *Mbnl1*$^{\Delta E3/\Delta E3}$ Bl6 congenic mice. (*A*) Splicing of Serca1, Mbnl1 and Mtmr3 among other Mbnl1 target pre-mRNAs is equivalent between *Mbnl1*$^{\Delta E3/\Delta E3}$ Bl6 and 129 muscles by RT-PCR, suggesting they are not molecular defects underlying the difference between backgrounds. Alternative exons are shown with black boxes. (*B*) Splicing of Tnnt3 and Ryr1 are different in *Mbnl1*$^{\Delta E3/\Delta E3}$ B6 and 129 muscles and correlate with myopathic changes. Inclusion ratio of Ryr1 exon 70 is >10 times lower in *Mbnl1*$^{\Delta E3/\Delta E3}$ Bl6, compared to 129, mice.

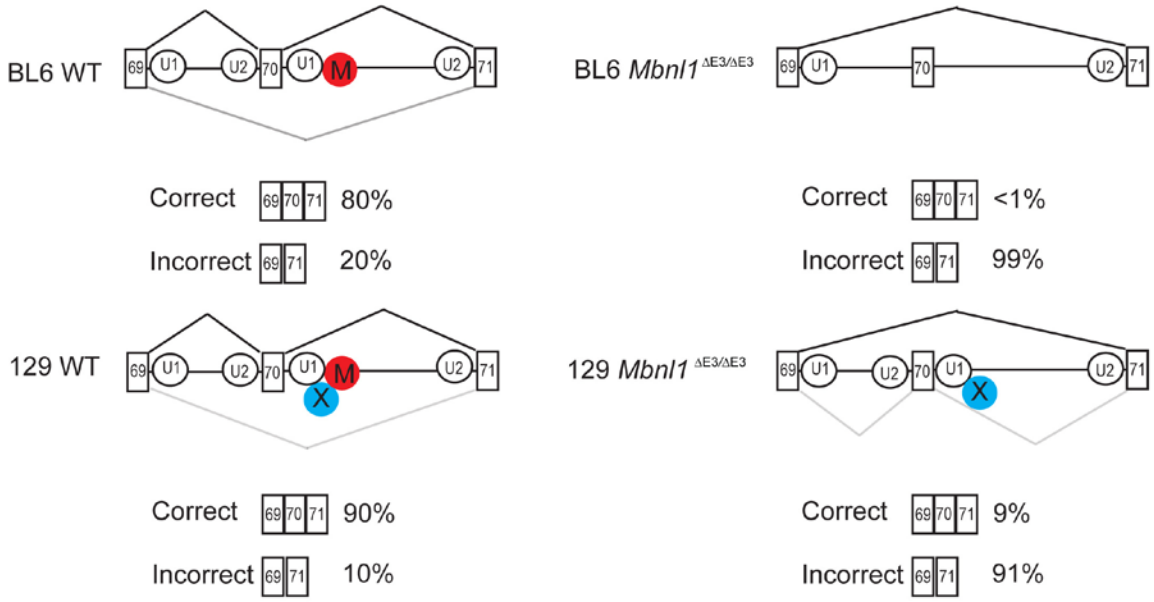


Figure 2-10. Model for association of MBNL1 and genetic modifier X with U1 snRNP. MBNL1 (red oval with M) and the genetic modifier X (blue oval with X) stabilize U1 snRNP (open oval with U1) binding at the 5' splice site of Ryr1 exon 70 (lines, introns; open boxes, exons). In the Bl6 background, splicing factor X is either absent or functionally compromised. Ratio of correct and incorrect transcripts of Ryr1 for each genotype is indicated with percentage.

# CHAPTER 3
# CONCLUDING REMARKS AND FUTURE DIRECTIONS

DM is a complex disease with multi-systemic clinical manifestations as well as remarkable variability among patients and the molecular etiology of this disease has been unclear for a long time. We hypothesized that loss of MBNL1 function is a primary pathogenic event in DM and we tested this idea by performing genetic complementation of *Mbnl1* in skeletal muscle of a poly(CUG) mouse model for DM. AAV-mediated gene transfer of *Mbnl1* was sufficient to rescue DM-associated phenotypes such as myotonia and missplicing in the TA muscle of the mouse even though it failed to reverse the muscle histopathology. Our results suggest that MBNL1 loss-of-function due to sequestration plays a major role in the development of myotonia and missplicing in DM. A revised experimental design, such as systemic delivery of untagged Mbnl1, will be required to test if muscle pathology is reversible. Alternatively, it will be interesting to see if genetic complementation of other *MBNL* family members, such as *MBNL2* and *MBNL3*, can rescue the structural changes of muscle induced by expression of toxic poly(CUG).

We also investigated the consequence of Mbnl1 loss-of-function by examining congenic (either Bl6 or 129) $Mbnl1^{\Delta E3/\Delta E3}$ mice. Our data demonstrated that Mbnl1 deficiency in mice leads to defects in multiple tissues and the severity depends on genetic background, which suggests that other factors are important to explain the variability and incomplete penetrance observed in DM patients. Our results also suggest that myotonia and myopathic changes in DM are two separable events and probably result from independent molecular mechanisms. We propose that disruption of calcium homeostasis due to missplicing of Ryr1 leads to the myopathy in DM. Future studies should investigate the

functional relevance of Ryr1 missplicing in vivo. Furthermore, analysis of congenic *Mbnl1*$^{\Delta E3/\Delta E3}$ mice identified defects in thymus and skin, which seem to involve hyperplasia of epithelial cells. Since there have been multiple case reports of tumors in individuals affected with DM, it will be interesting to investigate a potential role for MBNL1 dysregulation in tumorigenesis.

Our results clearly demonstrate that the MBNL1 loss-of-function model for DM is valid and explains many of the major pathogenesis events in DM. On the other hand, genetic factors seem to contribute to disease variability, which suggests that combinatorial therapeutic approaches will be required. Identification of the genetic modifier(s) that determines the disease severity will be an important contribution. We are hopeful that our data highlights the necessity for further studies on the molecular defects associated with less recognized disease-associated phenotypes as well as the mechanisms underlying the variability of this disease.

# CHAPTER 4
# MATERIALS AND METHODS

## Mice

The *HSA*$^{LR}$ 20b line was used for the study in Chapter 1. Intergenerational stability of the $(CTG)_{250}$ expansion was monitored by PCR with AmpliTaq Gold. The age of mice that were used for the experiments was typically 5 weeks old. Congenic *Mbnl1* knockout mice were generated by conventional backcrosses to inbred C57BL/6J or 129/Sv mice. *Mbnl1* genotyping was performed using genomic DNA from tail snips at 3 weeks of age. Tails (0.5cm) were lysed in 200 ul of 20 mM NaOH at 99°C for 1 hr and neutralized with same volume of 40 mM Tris-Cl (pH.8.0). Lysate (2 ul) was used to perform PCR. Primers used were MSS1382, MSS1383 and MSS884 and PCR cycles are as follows: 95°C for 30 sec, 60°C for 45 sec, and 68°C for 120 sec. 700bp band for PCR product is for WT allele and 800bp is for mutant allele.

## AAV2/1-mycMbnl1/41 Virus Preparation and Injection Protocol

A myc tag was added to the human MBNL1/41 ORF by using sequential PCR rounds with the same reverse primer (MSS1580) and the following four forward primers: 1, MSS1576; 2, MSS1577; 3, MSS1578; 4, MSS1579. Amplification for each round was performed for 25 cycles (98°C for 20 sec, 60°C for 30 sec, and 72°C for 90 sec). The PCR product was subcloned into pCR4-TOPO (Invitrogen, Carlsbad, CA) to create mycMBNL1/41. Human and mouse protein sequences vary by two amino acids in exon 5. Therefore, human cDNA was converted into a cDNA that encodes the mouse protein sequence by digestion of the mouse Mbnl1/41 ORF with HincII and HindIII followed by ligation into HincII/HindIII-digested mycMBNL1/41.

The mycMbnl1/41 cDNA was subcloned into SpeI/ClaI-cut pTR-UF12Δ (IRES-GFP deleted) to create pTR-UF12Δ-mycMbnl1/41. The plasmids pTR-UF12Δ-mycMbnl1/41 and pXYZ1 were used for virus preparation in HEK293 cells by using a two plasmid cotransfection protocol (114). The AAV2/1-mycMbnl1/41 vector was purified further by using a HiTrap Q column (GE Healthcare, Piscataway, NJ) (115), and the concentration ($1.24 \times 10^{13}$ vector genomes/ml) was determined by using a standardized real-time qPCR titration technique (116). The right TA muscles of 4- to 5-week-old *HSA*$^{LR}$ 20b mice were injected with one vector dose ($1 \times 10^{11}$ vector genomes in 30 μl of PBS) by using a 29-gauge needle.

AAV2/8-mycMbnl1/41 vector was prepared using similar protocol by University of Florida vector core laboratory except that pDG-AAV8 was used which contains the AAV8 capsid protein sequence. The concentration of virus was $1.3 \times 10^{13}$ vector genomes/ml. One day old *HSA*$^{LR}$ mice were anesthetized by hypothermia and administered with $2.5\text{-}5 \times 10^{11}$ particles (30 μl total volume) intravenously via the superficial temporal vein.

**Analysis of Mbnl1 Isoforms in Adult Muscle**

To determine the major Mbnl1 isoforms expressed in C57BL6/J skeletal muscle, total RNA was isolated from P2 hindlimb muscle and P28 quadriceps by using TRI Reagent (Sigma, St. Louis, MO). cDNA was generated by using 5 μg of RNA by random hexamer-primed reverse transcription by using SuperScript II (Invitrogen) followed by digestion with 0.2 units/μl RNase H (Invitrogen) at 37°C for 15 min. Mbnl1 isoforms were PCR-amplified through 35 cycles (95°C for 30 sec, 50°C for 30 sec, and 72°C for 90 sec) by using forward (MSS2161) and reverse (MSS2162) primers, and the product was cloned into

pCR4-TOPO. Multiple clones from P2 and P28 were randomly picked, and full-length cDNA coding sequences were obtained for both P2 ($n$ = 72) and P28 ($n$ = 81).

For immunological detection of Mbnl1, 9-month-old *HSA*$^{LR}$ tissues (tibialis anterior, gastrocnemius, quadriceps, cerebellum, heart, and lung) were homogenized in 50 mM Tris·Cl, pH = 6.8/1 mM EDTA/2% SDS/0.5 mM phenylmethylsulfonyl fluoride/5 μg/ml pepstatin A/1 μg/ml chymostatin/1 mM aminocaproic acid/1 mM *p*-aminobenzamidine/1 μg/ml leupeptin/2 μg/ml aprotinin. Homogenates were centrifuged at 16,000× *g* for 10 min, and supernatant proteins were fractionated on 12.5% SDS-polyacrylamide gels (50 μg protein per lane), electroblotted to nitrocellulose, immunoblotted, and visualized by ECL. Antibodies for immunoblotting included the rabbit anti-Mbnl1 polyclonal A2764 (1:1,000) and the anti-GAPDH monoclonal 6C5 (1:10,000; Novus Biologicals, Littleton, CO). The same procedure was performed for immunological detection of mycMbnl1/41 in AAV-transduced TA muscles.

**RNA Splicing**

For splicing analysis in cell culture, HEK293T cells were plated in six-well plates in DMEM (Invitrogen), supplemented with 10% FBS (Invitrogen) and 1% penicillin-streptomycin (Invitrogen). The next day, the cells were cotransfected with 1 μg of the Tnnt3 minigene and 10 ng of protein expression plasmids by using Lipofectamine 2000 (Invitrogen) according to the manufacturer's protocol. Protein and RNA were harvested 48 h after transfection. For analysis of GFP-fusion protein expression after transfection, proteins (20 μg per lane) were fractionated and detected by immunoblotting with anti-GFP (1:1,000; Roche, Indianapolis, IN) and anti-GAPDH mAb 6C5 (1:10,000). For RNA-

splicing analysis, first-strand cDNA was generated from total RNA by reverse transcription with 5 μg of total RNA and SuperScript II RNase H-RT (Invitrogen). Subsequent PCR (28 cycles at 95°C for 30 sec, 55°C for 30 sec, and 72°C for 30 sec) was performed by using 20% of the reverse transcription reaction as a template. Each PCR was spiked with 5 μCi (1 Ci = 37 GBq) of [$\alpha^{32}$P]-dCTP (PerkinElmer, Wellesley, MA). Tnnt3 minigene mRNA was analyzed by using exon 8 forward (MSS1956) and exon 9 reverse (MSS1938) primers. PCR products were resolved on 10% nondenaturing polyacrylamide gels followed by autoradiography with Biomax MS film (Eastman Kodak, Rochester, NY). Splicing shifts were measured by using a Pharox FX plus Molecular Imager (Bio-Rad, Hercules, CA).

Splicing patterns were monitored by radioactive RT-PCR as previously described (19). Primers used for Chapter 1 were as follows: Serca1, exon 21 forward (MSS2761) and exon 23 reverse (MSS2762); Cypher, exon 8 forward (MSS2763) and exon 13 reverse (MSS2764); Tnnt3, exon 2 and 3 overlapping forward (MSS1677) and exon 11 reverse (MSS1678); Clcn1, exon 6 forward (MSS2788) and exon 8 reverse (MSS1653); Capzb, exon 7 forward (MSS2765) and exon 9 reverse (MSS2766); Itgb1, exon 16 forward (MSS2767) and exon 18 reverse (MSS2768); myc-Mbnl1. forward primers in myc (MSS1579) and reverse primers in Mbnl1 exon 6 (MSS1656). Primers used for chapter 2 were as follows: Clcn1 exon 6 forward (MSS3513) and exon 7 reverse (MSS3514); Mbnl1 exon 6 forward (MA1) and exon 8 reverse (MA2); Mtmr3 exon 16 forward (MSS3825) and exon 18 reverse (MSS3826); Ryr1 exon 69 forward (MSS3890) and exon 71 reverse (MSS3891); Ryr1 exon 82 forward (MSS3892) and exon 84 reverse (MSS3893); Serca1 and Tnnt3 are same as above.

## Electromyography

Before electromyography, mice were anesthetized by i.p. using 100 mg/kg ketamine, 10 mg/kg xylazine, and 3 mg/kg acepromazine or 250 mg/kg 2,2,2 tribromoethanol. Electromyography on tibialis anterior and gastrocnemius muscles was performed as described (19) by using 30 gauge concentric needle electrodes and a minimum of 10 needle insertions for each muscle. For each time point (4, 12, 23, and 43 weeks after injection), at least 6 mice were evaluated, and both uninjected and injected TA, as well as gastrocnemius, muscles were tested. For congenic mice used in Chapter 2, numbers were between 4 and 6 and typical age at the time of analysis was 6 month old.

## Histology and Immunohistochemistry

Frozen sections (10 μm) of skeletal muscle were either prepared for routine H&E staining or immunostained by using antibodies against the ClC-1 C terminus (Alpha Diagnostic, San Antonio, TX) or the Mbnl1 C-terminal peptide (rabbit polyclonal antibody A2764) as described (36) with the following modifications. For Mbnl1, sections were fixed in 4% paraformaldehyde for 15 min at room temperature and permeabilized with 2% acetone in PBS for 5 min. For ClC-1, sections were unfixed. Primary antibody concentrations used were 1:10,000 for Mbnl1 and 1:50 for ClC-1. Secondary antibodies were goat anti-rabbit Alexa Fluor 488 and 546 (Invitrogen) at 1:400. Stacks of Z plane images were deconvolved by using a blind point spread function (117).

## Rotarod Test

Performance on an accelerating rotarod was tested for congenic mice to assess motor coordination. For four consecutive days, each subject was given four trials per day with a

minimum 10 min rest between trials. Revolutions per minute (rpm) were initially 4 rpm with a progressive increase to a maximum of 40 rpm for the first 2 min. Maximum trial length was 4 min. Latency to fall from the rotating rod was automatically detected and recorded by photo laser beams in the apparatus. Time to fall (Mean ± SEM) for each trial day was plotted.

### Analysis of T Cell Population by Flow Cytometry

Flow cytometry was performed by Dr. Changquing Xia in the Department of Pathology, University of Florida. Single thymocyte suspension was prepared using 10 μm cell strainer. After washing with PBS, centrifugated cell pellets were resuspended in red blood cell (RBC) lysis buffer to remove RBCs. After centrifugation, cell pellets were resuspended in washing buffer (PBS with 1% FBS). Cells were stained at 4°C for 1hr in washing buffer containing appropriate monoclonal antibodies. After a series of washing steps, thymocytes were subjected to flow cytometric anlysis on a Becton Dickinson FACScan apparatus. On the basis of forward angle light scatter gating, live cells were gated and analyzed according to their FSC and SSC profiles.

### *In Vitro* Force Measurements

*In vitro* force measurements were performed by Fan Ye in the Department of Physical therapy, University of Florida. Mice were anesthetized with isoflurane by inhalation and sacrificed by cervical dislocation. The soleus and EDL muscles were dissected with intact tendon and mounted horizontally in the organ bath of Ringer's solution gas-equilibrated with 95% $O_2$ and 5% $CO_2$ maintained at 25°C. Muscle tendons were tied with surgical silk thread to attach muscle to the experimental apparatus. The

muscles were adjusted to their optimal length to produce twitch force from supramaximal stimulation. Maximal titanic contraction force was determined by using a 120 Hz ,500ms pulse delivered by two parallel platinum plate electrodes. After force measurements, muscles were removed from bath and blotted on kimwipes twice and weighed for wet weight. Some of the muscles were mounted for histological analyses and were frozen in liquid nitrogen cold isopentane solution. Other muscles were snap frozen for molecular analyses and stored at -80℃.

**Neuromuscular Junction Staining**

TA muscles were dissected to stain neuromuscular junctions. After overnight incubation in 2% PFA at 4℃, muscle samples were washed in PBS. Then they were teased into ~0.3mm diameter bundles using a No.5 forceps. Myofiber bundles were permeabilized and blocked in 2% BSA 4% normal goat serum, 1% Triton X-100 in PBS for 1 hrs at room temperature and then incubated with Alexa Fluor 594 á-bungarotoxin (1:1,000) (Invitrogen B13423) in 1% Triton X-100 in PBS (wash buffer) for 1 hr at RT. Samples were washed with wash buffer 3 times before mounted on the microscope slide with a drop of DAPI solution (vector lab) and a No. 1 cover slip. Either confocal laser scanning microscope or regular Zeiss inverted microscope was used to take images of NMJs. For pre-synaptic staining, á-neurofillament (1:5,000 EnCor Biotechnology MCA-1H1) and á-SV2 (1:200 Iowa hybridoma core) antibodies were used.

**Calpain Activity Assay**

Biovision calpain activity assay kit (K240-100) was used to measure calpain activity in congenic quadriceps muscle extracts. Muscle protein extracts (50 μg) were incubated

with 10 µl of 10X reaction buffer and 5 µl of calpain substrates in total reaction volume of 100 µl at 37°C for 1 hr in the dark. Active calpain (2 µl) was added for positive control and 1µl of calpain inhibitor was added for negative control. Samples were transferred to 96 well plate and read in a fluorometer equipped with a 400nm excitation filter and 505nm emission filter. The activity is expressed as relative fluorescent unit (RFU) per mg protein of each sample.

**Ryr1 Minigene and Photocrosslinking Assay**

pSG5-Ryr1-E69.71 minigene was constructed by amplifying the mouse Ryr1 genomic region between exons 69 and 71 using MSS3923 and MSS3924 and inserting the PCR product into pSG5 (Stratagene, La Jolla, CA, USA) at the EcoRI site. For alternative construct containing only exon 70 and flanking 600nt, 600bp region crossing exon 70 was amplified using primers MSS4160 and MSS4161. And then it was inserted into pRSV-cTnt minigene to swap the cTnt genomic region using SalI and XbaI restriction enzyme sites.

Whole cell lysates for cross-linking was prepared as previously described (28). Briefly, HEK293T cells were transfected with 10 µg of pcDNA3-MBNL1mycHis and harvested in 48 hours. Cells are washed with PBS and resuspended in 250 µl of 20 mM HEPES–KOH (pH 8.0), 100 mM KCl, 0.1% IGEPAL and protease inhibitors. After sonication, lysates were centrifuged and supernatants were collected and glycerol was added to 20% of total volume. 600nt genomic region encompassing exon 70 of Ryr1 was labeled with ($\alpha$-$^{32}$P)-UTP (800 Ci/mmol) in the presence of 0.5 mM ATP and CTP, 0.02 mM GTP and UTP. Cross-linking was performed by incubating 0.1 pmol RNA with 15 µl of HEK293T whole cell lysate in 25 µl reactions containing 16 mM HEPES–KOH (pH 8.0),

65 mM potassium glutamate, 2 mM $Mg(OAC)_2$, 0.4 mM DTT, 0.16 mM EDTA, 20 mM creatine phosphate, 2 mM ATP and 16% glycerol (final concentration). Reactions were incubated at 30°C for 15 min, transferred to pre-chilled PCR caps on ice and photocrosslinked three times in Stratalinker (Stratagene, La Jolla, CA, USA) for 2.5 min with a 2 min interval between each irradiation. Samples were digested with 5 µg of RNase A for 20 min at 37°C and immunopurified using the anti-myc monoclonal antibody 9E10 pre-coated protein A Sepharose (Amersham). Purified proteins were fractionated on 12.5% SDS–PAGE gels followed by autoradiography. For splicing analysis of Ryr1 minigene, pRSV-Ryr1-E70 and protein expression plasmids were transfected into HEK293T and analyzed by RT-PCR as described above using primers MSS3497 and MSS3499.

| Primers used for genotyping Mbnl1 mouse | | |
|---|---|---|
| | MSS1382 | Fwd (5'-CTACGATGGCTGGCTGCAATATGCCTCACTGTAAG-3') |
| | MSS1383 | Rev (5'-CGTGGCAGACCCTTTGACACCGAATTTC-3') |
| Mbnl1 | MSS884 | Rev (5'-GGGTTGAATCTCGTTAGGGACACTGGGTGTCTGTAA-3') |
| Primers used for generation of mycMbnl1/41 | | |
| Myc 1st round | MSS1576 | Fwd (5'-GAGGAGGACCTGGCTGTTAGTGTCACACCAATTCGGGAC-3') |
| Myc 2nd round | MSS1577 | Fwd (5'-AAGCTGATCTCAGAGGAGGACCTGGCTGTTAGTGTCACA-3') |
| Myc 3rd round | MSS1578 | Fwd (5'-ATGGAGGAGCAGAAGCTGATCTCAGAGGAGGACCTGGCT-3') |
| Myc 4th round | MSS1579 | Fwd (5'-GGACTAGTCCATGGAGGAGCAGAAGCTGATCTCAGAGGA-3') |
| MBNL1 | MSS1580 | Exon12 rev (5'-CCATCGATGGCTACATCTGGGTAACATACTTGTGGCTAG-3') |
| Primers used for analysis of Mbnl1 isoforms | | |
| | MSS2161 | Exon3 fwd (5'-GGTTGGATTTGTTGGTTTCATTAAACATTTAAC-3') |
| Mbnl1 | MSS2162 | Exon13 rev (5'-ATATGTGGATGTCTTGTGGCTGAGGGA-3') |
| Primers used for RT-PCR | | |
| | MSS1956 | Exon8 fwd (5'-AGAATTGTAATACGACTCACTATAGGGC-3') |
| Tnnt3 minigene | MSS1938 | Exon9 rev (5'-GCTGCAATAAACAAGTTCTGCTTT-3') |
| | MSS2761 | Exon21 fwd (5'-GCTCATGGTCCTCAAGATCTCAC-3') |
| Serca1 | MSS2762 | Exon23 rev (5'-GGGTCAGTGCCTCAGCTTTG-3') |
| | MSS2763 | Exon5 fwd (5'-GGAAGATGAGGCTGATGAGTGG-3') |
| Cypher | MSS2764 | Exon10 rev (5'-TGCTGACAGTGGTAGTGCTCTTTC-3') |
| | MSS1677 | Exon2&3 fwd (5'-TCTGACGAGGAAACTGAACAAG-3') |
| Tnnt3 | MSS1678 | Exon11 rev (5'-TGTCAATGAGGGCTTGGAG-3') |
| | MSS2788 | Exon6 fwd (5'-TTCACATCGCCAGCATCTGTGC-3') |
| Clcn1 | MSS1653 | Exon8 rev (5'-CACGGAACACAAAGGCACTGAATGT-3') |
| | MSS2765 | Exon7 fwd (5'-GCACGCTGAATGAGATCTACTTTG-3') |
| Capzb | MSS2766 | Exon9 rev (5'-CCGGTTAGCGTGAAGCAGAG-3') |
| | MSS2767 | Exon16 fwd (5'-CCTACTGGTCCCGACATCATC-3') |
| Itgb1 | MSS2768 | Exon18 rev (5'-CTTCGGATTGACCACAGTTGTC-3') |
| | MSS1579 | Same as MSS1579 |
| MycMbnl1 | MSS1656 | Exon6 rev (5'-CCCTTGATGTAATCCATGCAGACAGTGA-3') |
| | MSS3513 | Exon6 fwd (5'-CTGAATGTGGCTGCAAAGAA-3') |
| Clcn1 | MSS3514 | Exon7 rev (5'-AAACAGCATTTCGAGCAACA-3') |
| | MSS3825 | Exon16 fwd (5'-CGACAGATAGAGTCTGGTCACCAGCA-3') |
| Mtmr3 | MSS3826 | Exon18 rev (5'-GCACTGTCACAGGCATAGCAGTGG-3') |
| | MSS3890 | Exon69 fwd (5'-GCGTGAAGAACAGAACTTCGTGGTC-3') |
| Ryr1 | MSS3891 | Exon71 rev (5'-CTTGGTGCGTTCCTGATCTGAGC-3') |
| | MSS3892 | Exon82 fwd (5'-CTTCGAGAGGCAGAACAAGGCAG-3') |
| Ryr1 | MSS3893 | Exon84 rev (5'-AACAGGTCCTGTGTGAACTCGTCATC-3') |
| Primers used for generation of Ryr1 minigene | | |
| | MSS3923 | Exon69 fwd (5'-GGCGAATTCAACTTTAAGCGTGAAGAACAGAACTTCGTGGTCCA-3') |
| | MSS3924 | Exon71 rev (5'-CCGGAATTCCAGGGCATAGCGGGCTTTGGCCA-3') |
| | MSS4160 | Intron69 fwd (5'-GCCGATATCGTGTCCACCCGTCTCCATCCTGT-3') |
| | MSS4161 | Intron70 rev (5'-GCCGATATCTGCATGGAGGAAAGCCAATGG-3') |
| | MSS3497 | Fwd (5'-AAACGCCATTTGACCATTCACCAC-3') |
| Ryr1 minigene | MSS3499 | Rev (5'-TGGAGCATAGCACTCTTCAGGTGCTG-3') |

Table 4-1. Sequence of primers

LIST OF REFERENCES


1. Haper, P.S. (2001) *Myotonic dystrophy*. Third ed. W.B. Saunders, London.

2. Brook, J.D., McCurrach, M.E., Harley, H.G., Buckler, A.J., Church, D., Aburatani, H., Hunter, K., Stanton, V.P., Thirion, J.P., Hudson, T. *et al.* (1992) Molecular basis of myotonic dystrophy: expansion of a trinucleotide (CTG) repeat at the 3' end of a transcript encoding a protein kinase family member. *Cell,* **68,** 799-808.

3. Liquori, C.L., Ricker, K., Moseley, M.L., Jacobsen, J.F., Kress, W., Naylor, S.L., Day, J.W. and Ranum, L.P. (2001) Myotonic dystrophy type 2 caused by a CCTG expansion in intron 1 of ZNF9. *Science (New York, N.Y,* **293,** 864-7.

4. Pearson, C.E., Nichol Edamura, K. and Cleary, J.D. (2005) Repeat instability: mechanisms of dynamic mutations. *Nat Rev Genet,* **6,** 729-42.

5. Thornton, C.A., Swanson, M.S. and Cooper, T.A. (2006) Chapter 3: The RNA-mediated disease process in myotonic dystrophy. In Ashizawa, T., Wells, R.D. (ed.), *Genetic instabilities and hereditary neurological diseases.* 2nd ed. Elsevier-academic press, San Diego.

6. Otten, A.D. and Tapscott, S.J. (1995) Triplet repeat expansion in myotonic dystrophy alters the adjacent chromatin structure. *Proceedings of the National Academy of Sciences of the United States of America,* **92,** 5465-9.

7. O'Rourke, J.R. and Swanson, M.S. (2009) Mechanisms of RNA-mediated disease. *The Journal of biological chemistry,* **284,** 7419-23.

8. Ranum, L.P. and Day, J.W. (2004) Pathogenic RNA repeats: an expanding role in genetic disease. *Trends Genet,* **20,** 506-12.

9. Berul, C.I., Maguire, C.T., Aronovitz, M.J., Greenwood, J., Miller, C., Gehrmann, J., Housman, D., Mendelsohn, M.E. and Reddy, S. (1999) DMPK dosage alterations result in atrioventricular conduction abnormalities in a mouse myotonic dystrophy model. *The Journal of clinical investigation,* **103,** R1-7.

10. Jansen, G., Groenen, P.J., Bachner, D., Jap, P.H., Coerwinkel, M., Oerlemans, F., van den Broek, W., Gohlsch, B., Pette, D., Plomp, J.J. *et al.* (1996) Abnormal myotonic dystrophy protein kinase levels produce only mild myopathy in mice. *Nature genetics,* **13,** 316-24.

11. Sarkar, P.S., Appukuttan, B., Han, J., Ito, Y., Ai, C., Tsai, W., Chai, Y., Stout, J.T. and Reddy, S. (2000) Heterozygous loss of Six5 in mice is sufficient to cause ocular cataracts. *Nature genetics,* **25,** 110-4.

12. Miller, J.W., Urbinati, C.R., Teng-Umnuay, P., Stenberg, M.G., Byrne, B.J., Thornton, C.A. and Swanson, M.S. (2000) Recruitment of human muscleblind proteins to (CUG)(n) expansions associated with myotonic dystrophy. *Embo J,* **19,** 4439-48.

13. Davis, B.M., McCurrach, M.E., Taneja, K.L., Singer, R.H. and Housman, D.E. (1997) Expansion of a CUG trinucleotide repeat in the 3' untranslated region of myotonic dystrophy protein kinase transcripts results in nuclear retention of transcripts. *Proceedings of the National Academy of Sciences of the United States of America,* **94,** 7388-93.

14. Taneja, K.L., McCurrach, M., Schalling, M., Housman, D. and Singer, R.H. (1995) Foci of trinucleotide repeat transcripts in nuclei of myotonic dystrophy cells and tissues. *The Journal of cell biology,* **128,** 995-1002.

15. Michalowski, S., Miller, J.W., Urbinati, C.R., Paliouras, M., Swanson, M.S. and Griffith, J. (1999) Visualization of double-stranded RNAs from the myotonic dystrophy protein kinase gene and interactions with CUG-binding protein. *Nucleic acids research,* **27,** 3534-42.

16. Mooers, B.H., Logue, J.S. and Berglund, J.A. (2005) The structural basis of myotonic dystrophy from the crystal structure of CUG repeats. *Proceedings of the National Academy of Sciences of the United States of America,* **102,** 16626-31.

17. Mankodi, A., Logigian, E., Callahan, L., McClain, C., White, R., Henderson, D., Krym, M. and Thornton, C.A. (2000) Myotonic dystrophy in transgenic mice expressing an expanded CUG repeat. *Science (New York, N.Y,* **289,** 1769-73.

18. Ho, T.H., Charlet, B.N., Poulos, M.G., Singh, G., Swanson, M.S. and Cooper, T.A. (2004) Muscleblind proteins regulate alternative splicing. *Embo J,* **23,** 3103-12.

19. Kanadia, R.N., Johnstone, K.A., Mankodi, A., Lungu, C., Thornton, C.A., Esson, D., Timmers, A.M., Hauswirth, W.W. and Swanson, M.S. (2003) A muscleblind knockout model for myotonic dystrophy. *Science (New York, N.Y,* **302,** 1978-80.

20. Philips, A.V., Timchenko, L.T. and Cooper, T.A. (1998) Disruption of splicing regulated by a CUG-binding protein in myotonic dystrophy. *Science (New York, N.Y,* **280,** 737-41.

21. Dansithong, W., Paul, S., Comai, L. and Reddy, S. (2005) MBNL1 is the primary determinant of focus formation and aberrant insulin receptor splicing in DM1. *The Journal of biological chemistry,* **280,** 5773-80.

22. Savkur, R.S., Philips, A.V. and Cooper, T.A. (2001) Aberrant regulation of insulin receptor alternative splicing is associated with insulin resistance in myotonic dystrophy. *Nature genetics,* **29,** 40-7.

23. Timchenko, N.A., Cai, Z.J., Welm, A.L., Reddy, S., Ashizawa, T. and Timchenko, L.T. (2001) RNA CUG repeats sequester CUGBP1 and alter protein levels and activity of CUGBP1. *The Journal of biological chemistry,* **276,** 7820-6.

24. Kuyumcu-Martinez, N.M., Wang, G.S. and Cooper, T.A. (2007) Increased steady-state levels of CUGBP1 in myotonic dystrophy 1 are due to PKC-mediated hyperphosphorylation. *Molecular cell,* **28,** 68-78.

25. Fardaei, M., Larkin, K., Brook, J.D. and Hamshere, M.G. (2001) In vivo co-localisation of MBNL protein with DMPK expanded-repeat transcripts. *Nucleic acids research,* **29,** 2766-71.

26. Mankodi, A., Teng-Umnuay, P., Krym, M., Henderson, D., Swanson, M. and Thornton, C.A. (2003) Ribonuclear inclusions in skeletal muscle in myotonic dystrophy types 1 and 2. *Ann Neurol,* **54,** 760-8.

27. Mankodi, A., Urbinati, C.R., Yuan, Q.P., Moxley, R.T., Sansone, V., Krym, M., Henderson, D., Schalling, M., Swanson, M.S. and Thornton, C.A. (2001) Muscleblind localizes to nuclear foci of aberrant RNA in myotonic dystrophy types 1 and 2. *Human molecular genetics,* **10,** 2165-70.

28. Yuan, Y., Compton, S.A., Sobczak, K., Stenberg, M.G., Thornton, C.A., Griffith, J.D. and Swanson, M.S. (2007) Muscleblind-like 1 interacts with RNA hairpins in splicing target and pathogenic RNAs. *Nucleic acids research,* **35,** 5474-86.

29. Timchenko, L.T., Miller, J.W., Timchenko, N.A., DeVore, D.R., Datar, K.V., Lin, L., Roberts, R., Caskey, C.T. and Swanson, M.S. (1996) Identification of a (CUG)n triplet repeat RNA-binding protein and its expression in myotonic dystrophy. *Nucleic acids research,* **24,** 4407-14.

30. Fardaei, M., Rogers, M.T., Thorpe, H.M., Larkin, K., Hamshere, M.G., Harper, P.S. and Brook, J.D. (2002) Three proteins, MBNL, MBLL and MBXL, co-localize in vivo with nuclear foci of expanded-repeat transcripts in DM1 and DM2 cells. *Human molecular genetics,* **11,** 805-14.

31. Kanadia, R.N., Urbinati, C.R., Crusselle, V.J., Luo, D., Lee, Y.J., Harrison, J.K., Oh, S.P. and Swanson, M.S. (2003) Developmental expression of mouse muscleblind genes Mbnl1, Mbnl2 and Mbnl3. *Gene Expr Patterns,* **3,** 459-62.

32. Hao, M., Akrami, K., Wei, K., De Diego, C., Che, N., Ku, J.H., Tidball, J., Graves, M.C., Shieh, P.B. and Chen, F. (2008) Muscleblind-like 2 (Mbnl2) -deficient mice as a model for myotonic dystrophy. *Dev Dyn,* **237,** 403-10.

33. Lin, X., Miller, J.W., Mankodi, A., Kanadia, R.N., Yuan, Y., Moxley, R.T., Swanson, M.S. and Thornton, C.A. (2006) Failure of MBNL1-dependent post-natal splicing transitions in myotonic dystrophy. *Human molecular genetics,* **15,** 2087-97.

34. Ho, T.H., Bundman, D., Armstrong, D.L. and Cooper, T.A. (2005) Transgenic mice expressing CUG-BP1 reproduce splicing mis-regulation observed in myotonic dystrophy. *Human molecular genetics,* **14,** 1539-47.

35. Charlet, B.N., Savkur, R.S., Singh, G., Philips, A.V., Grice, E.A. and Cooper, T.A. (2002) Loss of the muscle-specific chloride channel in type 1 myotonic dystrophy due to misregulated alternative splicing. *Molecular cell,* **10,** 45-53.

36. Mankodi, A., Takahashi, M.P., Jiang, H., Beck, C.L., Bowers, W.J., Moxley, R.T., Cannon, S.C. and Thornton, C.A. (2002) Expanded CUG repeats trigger aberrant splicing of ClC-1 chloride channel pre-mRNA and hyperexcitability of skeletal muscle in myotonic dystrophy. *Molecular cell,* **10,** 35-44.

37. Lueck, J.D., Lungu, C., Mankodi, A., Osborne, R.J., Welle, S.L., Dirksen, R.T. and Thornton, C.A. (2007) Chloride channelopathy in myotonic dystrophy resulting from loss of posttranscriptional regulation for CLCN1. *American journal of physiology,* **292,** C1291-7.

38. Lueck, J.D., Mankodi, A., Swanson, M.S., Thornton, C.A. and Dirksen, R.T. (2007) Muscle chloride channel dysfunction in two mouse models of myotonic dystrophy. *The Journal of general physiology,* **129,** 79-94.

39. Wheeler, T.M., Lueck, J.D., Swanson, M.S., Dirksen, R.T. and Thornton, C.A. (2007) Correction of ClC-1 splicing eliminates chloride channelopathy and myotonia in mouse models of myotonic dystrophy. *The Journal of clinical investigation,* **117,** 3952-7.

40. Kim, D.H., Langlois, M.A., Lee, K.B., Riggs, A.D., Puymirat, J. and Rossi, J.J. (2005) HnRNP H inhibits nuclear export of mRNA containing expanded CUG repeats and a distal branch point sequence. *Nucleic acids research,* **33,** 3866-74.

41. Ebralidze, A., Wang, Y., Petkova, V., Ebralidse, K. and Junghans, R.P. (2004) RNA leaching of transcription factors disrupts transcription in myotonic dystrophy. *Science (New York, N.Y,* **303,** 383-7.

42. Meola, G. and Sansone, V. (2004) Treatment in myotonia and periodic paralysis. *Rev Neurol (Paris),* **160,** S55-69.

43. Di Prospero, N.A. and Fischbeck, K.H. (2005) Therapeutics development for triplet repeat expansion diseases. *Nat Rev Genet,* **6,** 756-65.

44. Wheeler, T.M., Sobczak, K., Lueck, J.D., Osborne, R.J., Lin, X., Dirksen, R.T. and Thornton, C.A. (2009) Reversal of RNA dominance by displacement of protein sequestered on triplet repeat RNA. *Science (New York, N.Y,* **325,** 336-9.

45. Mulders, S.A., van den Broek, W.J., Wheeler, T.M., Croes, H.J., van Kuik-Romeijn, P., de Kimpe, S.J., Furling, D., Platenburg, G.J., Gourdon, G., Thornton, C.A. *et al.* (2009) Triplet-repeat oligonucleotide-mediated reversal of RNA toxicity in myotonic dystrophy. *Proceedings of the National Academy of Sciences of the United States of America,* **106,** 13915-20.

46. Warf, M.B., Nakamori, M., Matthys, C.M., Thornton, C.A. and Berglund, J.A. (2009) Pentamidine reverses the splicing defects associated with myotonic dystrophy. *Proceedings of the National Academy of Sciences of the United States of America,* **106,** 18551-6.

47. Flotte, T.R. and Carter, B.J. (1995) Adeno-associated virus vectors for gene therapy. *Gene Ther,* **2,** 357-62.

48. Flotte, T.R., Brantly, M.L., Spencer, L.T., Byrne, B.J., Spencer, C.T., Baker, D.J. and Humphries, M. (2004) Phase I trial of intramuscular injection of a recombinant adeno-associated virus alpha 1-antitrypsin (rAAV2-CB-hAAT) gene vector to AAT-deficient adults. *Hum Gene Ther,* **15,** 93-128.

49. Flotte, T.R., Zeitlin, P.L., Reynolds, T.C., Heald, A.E., Pedersen, P., Beck, S., Conrad, C.K., Brass-Ernst, L., Humphries, M., Sullivan, K. *et al.* (2003) Phase I trial of intranasal and endobronchial administration of a recombinant adeno-associated virus serotype 2 (rAAV2)-CFTR vector in adult cystic fibrosis patients: a two-part clinical study. *Hum Gene Ther,* **14,** 1079-88.

50. Manno, C.S., Chew, A.J., Hutchison, S., Larson, P.J., Herzog, R.W., Arruda, V.R., Tai, S.J., Ragni, M.V., Thompson, A., Ozelo, M. *et al.* (2003) AAV-mediated factor IX gene transfer to skeletal muscle in patients with severe hemophilia B. *Blood,* **101,** 2963-72.

51. Moss, R.B., Rodman, D., Spencer, L.T., Aitken, M.L., Zeitlin, P.L., Waltz, D., Milla, C., Brody, A.S., Clancy, J.P., Ramsey, B. *et al.* (2004) Repeated adeno-associated virus serotype 2 aerosol-mediated cystic fibrosis transmembrane regulator gene transfer to the lungs of patients with cystic fibrosis: a multicenter, double-blind, placebo-controlled trial. *Chest,* **125,** 509-21.

52. Ho, T.H., Savkur, R.S., Poulos, M.G., Mancini, M.A., Swanson, M.S. and Cooper, T.A. (2005) Colocalization of muscleblind with RNA foci is separable from mis-regulation of alternative splicing in myotonic dystrophy. *J Cell Sci,* **118,** 2923-33.

53. Kino, Y., Mori, D., Oma, Y., Takeshita, Y., Sasagawa, N. and Ishiura, S. (2004) Muscleblind protein, MBNL1/EXP, binds specifically to CHHG repeats. *Human molecular genetics,* **13,** 495-507.

54. Xiao, X., Li, J., Tsao, Y.P., Dressman, D., Hoffman, E.P. and Watchko, J.F. (2000) Full functional rescue of a complete muscle (TA) in dystrophic hamsters by adeno-associated virus vector-directed gene therapy. *J Virol,* **74,** 1436-42.

55. Zhou, Q., Chu, P.H., Huang, C., Cheng, C.F., Martone, M.E., Knoll, G., Shelton, G.D., Evans, S. and Chen, J. (2001) Ablation of Cypher, a PDZ-LIM domain Z-line protein, causes a severe form of congenital myopathy. *The Journal of cell biology,* **155,** 605-12.

56. Selcen, D. and Engel, A.G. (2005) Mutations in ZASP define a novel form of muscular dystrophy in humans. *Ann Neurol,* **57,** 269-76.

57. Kimura, T., Nakamori, M., Lueck, J.D., Pouliquin, P., Aoike, F., Fujimura, H., Dirksen, R.T., Takahashi, M.P., Dulhunty, A.F. and Sakoda, S. (2005) Altered mRNA splicing of the skeletal muscle ryanodine receptor and sarcoplasmic/endoplasmic reticulum Ca2+-ATPase in myotonic dystrophy type 1. *Human molecular genetics,* **14,** 2189-200.

58. Wang, Z., Zhu, T., Qiao, C., Zhou, L., Wang, B., Zhang, J., Chen, C., Li, J. and Xiao, X. (2005) Adeno-associated virus serotype 8 efficiently delivers genes to muscle and heart. *Nat Biotechnol,* **23,** 321-8.

59. Adereth, Y., Dammai, V., Kose, N., Li, R. and Hsu, T. (2005) RNA-dependent integrin alpha3 protein localization regulated by the Muscleblind-like protein MLP1. *Nature cell biology,* **7,** 1240-7.

60. Hunter, A., Tsilfidis, C., Mettler, G., Jacob, P., Mahadevan, M., Surh, L. and Korneluk, R. (1992) The correlation of age of onset with CTG trinucleotide repeat amplification in myotonic dystrophy. *Journal of medical genetics,* **29,** 774-9.

61. Harper, P. (2002) *Myotonic Dystrophy: The Facts*. Oxford University Press, USA.

62. Mueller, C.M., Hilbert, J.E., Martens, W., Thornton, C.A., Moxley, R.T., 3rd and Greene, M.H. (2009) Hypothesis: neoplasms in myotonic dystrophy. *Cancer Causes Control.*

63. Harper, P.S. (1972) Calcifying epithelioma of Malherbe. Association with myotonic muscular dystrophy. *Archives of dermatology,* **106,** 41-4.

64. Murakami, N., Kamimoto, K., Sakurai, N., Kawai, K. and Muroga, T. (1986) [Myotonic dystrophy associated with multiple calcifying epithelioma of Malherbe]. *Rinsho shinkeigaku = Clinical neurology,* **26,** 505-8.

65. Zemtsov, A. (2009) Association between basal, squamous cell carcinomas, dysplastic nevi and myotonic muscular dystrophy indicates an important role of RNA-binding proteins in development of human skin cancer. *Archives of dermatological research*.

66. Gomes-Pereira, M., Foiry, L., Nicole, A., Huguet, A., Junien, C., Munnich, A. and Gourdon, G. (2007) CTG trinucleotide repeat "big jumps": large expansions, small mice. *PLoS genetics,* **3,** e52.

67. Seznec, H., Agbulut, O., Sergeant, N., Savouret, C., Ghestem, A., Tabti, N., Willer, J.C., Ourth, L., Duros, C., Brisson, E. *et al.* (2001) Mice transgenic for the human myotonic dystrophy region with expanded CTG repeats display muscular and brain abnormalities. *Human molecular genetics,* **10,** 2717-26.

68. Seznec, H., Lia-Baldini, A.S., Duros, C., Fouquet, C., Lacroix, C., Hofmann-Radvanyi, H., Junien, C. and Gourdon, G. (2000) Transgenic mice carrying large human genomic sequences with expanded CTG repeat mimic closely the DM CTG repeat intergenerational and somatic instability. *Human molecular genetics,* **9,** 1185-94.

69. Wang, G.S., Kearney, D.L., De Biasi, M., Taffet, G. and Cooper, T.A. (2007) Elevation of RNA-binding protein CUGBP1 is an early event in an inducible heart-specific mouse model of myotonic dystrophy. *The Journal of clinical investigation,* **117,** 2802-11.

70. Orengo, J.P., Chambon, P., Metzger, D., Mosier, D.R., Snipes, G.J. and Cooper, T.A. (2008) Expanded CTG repeats within the DMPK 3' UTR causes severe skeletal muscle wasting in an inducible mouse model for myotonic dystrophy. *Proceedings of the National Academy of Sciences of the United States of America,* **105,** 2646-51.

71. Doetschman, T. (2009) Influence of genetic background on genetically engineered mouse phenotypes. *Methods in molecular biology (Clifton, N.J,* **530,** 423-33.

72. Lathe, R. (1996) Mice, gene targeting and behaviour: more than just genetic background. *Trends in neurosciences,* **19,** 183-6; discussion 188-9.

73. Crawley, J.N., Belknap, J.K., Collins, A., Crabbe, J.C., Frankel, W., Henderson, N., Hitzemann, R.J., Maxson, S.C., Miner, L.L., Silva, A.J. *et al*. (1997) Behavioral phenotypes of inbred mouse strains: implications and recommendations for molecular studies. *Psychopharmacology,* **132,** 107-24.

74. Stevens, L.C. (1973) A new inbred subline of mice (129-terSv) with a high incidence of spontaneous congenital testicular teratomas. *Journal of the National Cancer Institute,* **50,** 235-42.

75. Andrews, A.G., Dysko, R.C., Spilman, S.C., Kunkel, R.G., Brammer, D.W. and Johnson, K.J. (1994) Immune complex vasculitis with secondary ulcerative dermatitis in aged C57BL/6NNia mice. *Veterinary pathology,* **31,** 293-300.

76. Dimai, H.P., Linkhart, T.A., Linkhart, S.G., Donahue, L.R., Beamer, W.G., Rosen, C.J., Farley, J.R. and Baylink, D.J. (1998) Alkaline phosphatase levels and osteoprogenitor cell numbers suggest bone formation may contribute to peak bone density differences between two inbred strains of mice. *Bone,* **22,** 211-6.

77. Smith, R.S., Roderick, T.H. and Sundberg, J.P. (1994) Microphthalmia and associated abnormalities in inbred black mice. *Laboratory animal science,* **44,** 551-60.

78. Leonard, J.R., Klocke, B.J., D'Sa, C., Flavell, R.A. and Roth, K.A. (2002) Strain-dependent neurodevelopmental abnormalities in caspase-3-deficient mice. *Journal of neuropathology and experimental neurology,* **61,** 673-7.

79. Lloret, A., Dragileva, E., Teed, A., Espinola, J., Fossale, E., Gillis, T., Lopez, E., Myers, R.H., MacDonald, M.E. and Wheeler, V.C. (2006) Genetic background modifies nuclear mutant huntingtin accumulation and HD CAG repeat instability in Huntington's disease knock-in mice. *Human molecular genetics,* **15,** 2015-24.

80. Davies, J.C., Turner, M.W. and Klein, N. (2004) Impaired pulmonary status in cystic fibrosis adults with two mutated MBL-2 alleles. *Eur Respir J,* **24,** 798-804.

81. Olesen, H.V., Jensenius, J.C., Steffensen, R., Thiel, S. and Schiotz, P.O. (2006) The mannan-binding lectin pathway and lung disease in cystic fibrosis--disfunction of mannan-binding lectin-associated serine protease 2 (MASP-2) may be a major modifier. *Clinical immunology (Orlando, Fla,* **121,** 324-31.

82. Yadava, R.S., Frenzel-McCardell, C.D., Yu, Q., Srinivasan, V., Tucker, A.L., Puymirat, J., Thornton, C.A., Prall, O.W., Harvey, R.P. and Mahadevan, M.S. (2008) RNA toxicity in myotonic muscular dystrophy induces NKX2-5 expression. *Nature genetics,* **40,** 61-8.

83. Anderson, G., Lane, P.J. and Jenkinson, E.J. (2007) Generating intrathymic microenvironments to establish T-cell tolerance. *Nature reviews,* **7,** 954-63.

84. Takahama, Y. (2006) Journey through the thymus: stromal guides for T-cell development and selection. *Nature reviews,* **6,** 127-35.

85. Heller, A.H., Eicher, E.M., Hallett, M. and Sidman, R.L. (1982) Myotonia, a new inherited muscle disease in mice. *J Neurosci,* **2,** 924-33.

86. van der Laarse, W.J., Diegenbach, P.C. and Maslam, S. (1984) Quantitative histochemistry of three mouse hind-limb muscles: the relationship between calcium-stimulated myofibrillar ATPase and succinate dehydrogenase activities. *The Histochemical journal,* **16,** 529-41.

87. Hughes, S.M., Chi, M.M., Lowry, O.H. and Gundersen, K. (1999) Myogenin induces a shift of enzyme activity from glycolytic to oxidative metabolism in muscles of transgenic mice. *The Journal of cell biology,* **145,** 633-42.

88. Cumsky, M.G., McEwen, J.E., Ko, C. and Poyton, R.O. (1983) Nuclear genes for mitochondrial proteins. Identification and isolation of a structural gene for subunit V of yeast cytochrome c oxidase. *The Journal of biological chemistry,* **258,** 13418-21.

89. Rafael, J.A., Townsend, E.R., Squire, S.E., Potter, A.C., Chamberlain, J.S. and Davies, K.E. (2000) Dystrophin and utrophin influence fiber type composition and post-synaptic membrane structure. *Human molecular genetics,* **9,** 1357-67.

90. Kimura, T., Lueck, J.D., Harvey, P.J., Pace, S.M., Ikemoto, N., Casarotto, M.G., Dirksen, R.T. and Dulhunty, A.F. (2009) Alternative splicing of RyR1 alters the efficacy of skeletal EC coupling. *Cell calcium,* **45,** 264-74.

91. Gilboa-Geffen, A., Lacoste, P.P., Soreq, L., Cizeron-Clairac, G., Le Panse, R., Truffault, F., Shaked, I., Soreq, H. and Berrih-Aknin, S. (2007) The thymic theme of acetylcholinesterase splice variants in myasthenia gravis. *Blood,* **109,** 4383-91.

92. Peters, T., Ausmeier, K., Dildrop, R. and Ruther, U. (2002) The mouse Fused toes (Ft) mutation is the result of a 1.6-Mb deletion including the entire Iroquois B gene cluster. *Mamm Genome,* **13,** 186-8.

93. Volkmann, A., Doffinger, R., Ruther, U. and Kyewski, B.A. (1996) Insertional mutagenesis affecting programmed cell death leads to thymic hyperplasia and altered thymopoiesis. *J Immunol,* **156,** 136-45.

94. Ting, K.M., Rothaupt, D., McCormick, T.S., Hammerberg, C., Chen, G., Gilliam, A.C., Stevens, S., Culp, L. and Cooper, K.D. (2000) Overexpression of the oncofetal Fn variant containing the EDA splice-in segment in the dermal-epidermal junction of psoriatic uninvolved skin. *The Journal of investigative dermatology,* **114,** 706-11.

95. Olsen, N.J., Olson, G., Viselli, S.M., Gu, X. and Kovacs, W.J. (2001) Androgen receptors in thymic epithelium modulate thymus size and thymocyte development. *Endocrinology,* **142,** 1278-83.

96. Papadaki, O., Milatos, S., Grammenoudi, S., Mukherjee, N., Keene, J.D. and Kontoyiannis, D.L. (2009) Control of thymic T cell maturation, deletion and egress by the RNA-binding protein HuR. *J Immunol,* **182,** 6779-88.

97. Wang, H.Y., Xu, X., Ding, J.H., Bermingham, J.R., Jr. and Fu, X.D. (2001) SC35 plays a role in T cell development and alternative splicing of CD45. *Molecular cell,* **7,** 331-42.

98. Carlin, L. and Biller, J. (1981) Myotonic dystrophy and thymoma. *Journal of neurology, neurosurgery, and psychiatry,* **44,** 852-3.

99. Kudva, G.C., Maliekel, K., Kim, H.J., Naunheim, K.S., Stolar, C., Fletcher, J.W. and Puri, S. (2002) Thymoma and myotonic dystrophy: successful treatment with chemotherapy and radiation: case report and review of the literature. *Chest,* **121,** 2061-3.

100. Kuroiwa, Y., Yamada, A., Ikebe, K., Kosaka, K., Sugita, H. and Murakami, T. (1981) Myotonic dystrophy and thymoma: a necropsy case report. *Journal of neurology, neurosurgery, and psychiatry,* **44,** 173-5.

101. Xia, J., Urabe, K., Moroi, Y., Koga, T., Duan, H., Li, Y. and Furue, M. (2006) beta-Catenin mutation and its nuclear localization are confirmed to be frequent causes of Wnt signaling pathway activation in pilomatricomas. *Journal of dermatological science,* **41,** 67-75.

102. Bassel-Duby, R. and Olson, E.N. (2006) Signaling pathways in skeletal muscle remodeling. *Annual review of biochemistry,* **75,** 19-37.

103. Reininghaus, J., Fuchtbauer, E.M., Bertram, K. and Jockusch, H. (1988) The myotonic mouse mutant ADR: physiological and histochemical properties of muscle. *Muscle & nerve,* **11,** 433-9.

104. van Lunteren, E., Pollarine, J. and Moyer, M. (2007) Isotonic contractile impairment due to genetic CLC-1 chloride channel deficiency in myotonic mouse diaphragm muscle. *Experimental physiology,* **92,** 717-29.

105. Panaite, P.A., Gantelet, E., Kraftsik, R., Gourdon, G., Kuntzer, T. and Barakat-Walter, I. (2008) Myotonic dystrophy transgenic mice exhibit pathologic abnormalities in diaphragm neuromuscular junctions and phrenic nerves. *Journal of neuropathology and experimental neurology,* **67,** 763-72.

106. Wheeler, T.M., Krym, M.C. and Thornton, C.A. (2007) Ribonuclear foci at the neuromuscular junction in myotonic dystrophy type 1. *Neuromuscul Disord,* **17,** 242-7.

107. Boer, J.M., de Meijer, E.J., Mank, E.M., van Ommen, G.B. and den Dunnen, J.T. (2002) Expression profiling in stably regenerating skeletal muscle of dystrophin-deficient mdx mice. *Neuromuscul Disord,* **12 Suppl 1,** S118-24.

108. Tanabe, Y., Esaki, K. and Nomura, T. (1986) Skeletal muscle pathology in X chromosome-linked muscular dystrophy (mdx) mouse. *Acta neuropathologica,* **69,** 91-5.

109. Treves, S., Anderson, A.A., Ducreux, S., Divet, A., Bleunven, C., Grasso, C., Paesante, S. and Zorzato, F. (2005) Ryanodine receptor 1 mutations, dysregulation of calcium homeostasis and neuromuscular disorders. *Neuromuscul Disord,* **15,** 577-87.

110. Buchner, D.A., Trudeau, M. and Meisler, M.H. (2003) SCNM1, a putative RNA splicing factor that modifies disease severity in mice. *Science (New York, N.Y,* **301,** 967-9.

111. Kearney, J.A., Buchner, D.A., De Haan, G., Adamska, M., Levin, S.I., Furay, A.R., Albin, R.L., Jones, J.M., Montal, M., Stevens, M.J. *et al.* (2002) Molecular and pathological effects of a modifier gene on deficiency of the sodium channel Scn8a (Na(v)1.6). *Human molecular genetics,* **11,** 2765-75.

112. Sprunger, L.K., Escayg, A., Tallaksen-Greene, S., Albin, R.L. and Meisler, M.H. (1999) Dystonia associated with mutation of the neuronal sodium channel Scn8a and identification of the modifier locus Scnm1 on mouse chromosome 3. *Human molecular genetics,* **8,** 471-9.

113. Howell, V.M., Jones, J.M., Bergren, S.K., Li, L., Billi, A.C., Avenarius, M.R. and Meisler, M.H. (2007) Evidence for a direct role of the disease modifier SCNM1 in splicing. *Human molecular genetics,* **16,** 2506-16.

114. Harris, J.D., Beattie, S.G. and Dickson, J.G. (2003) Novel tools for production and purification of recombinant adeno-associated viral vectors. *Methods Mol Med,* **76,** 255-67.

115. Zolotukhin, S., Potter, M., Zolotukhin, I., Sakai, Y., Loiler, S., Fraites, T.J., Jr., Chiodo, V.A., Phillipsberg, T., Muzyczka, N., Hauswirth, W.W. *et al.* (2002) Production and purification of serotype 1, 2, and 5 recombinant adeno-associated viral vectors. *Methods,* **28,** 158-67.

116. Veldwijk, M.R., Topaly, J., Laufs, S., Hengge, U.R., Wenz, F., Zeller, W.J. and Fruehauf, S. (2002) Development and optimization of a real-time quantitative PCR-based method for the titration of AAV-2 vector stocks. *Mol Ther,* **6,** 272-8.

117. Holmes, T.J. and O'Connor, N.J. (2000) Blind deconvolution of 3D transmitted light brightfield micrographs. *J Microsc,* **200,** 114-27.

# BIOGRAPHICAL SKETCH

Jihae Shin was born in Inchon, Korea in 1979. She is the eldest born to Bokyeong Heo and Bukyun Shin. Jihae graduated from Incheon Science High School in 1998, and attended Seoul National University from 1998-2003, where she studied biological sciences and earned a Bachelor of Science in Biology. She was also a student at the University of Tokyo, Japan from 2000-2001, where she had her first research experience under Dr. Ryoichi Matsuda. After graduation, Jihae moved to United States to join the interdisciplinary program in biomedical sciences at the University of Florida, College of Medicine in Gainesville, Florida. She did her graduate work in Dr. Maurice Swanson's laboratory of the Molecular Genetics and Microbiology Department and completed her Ph.D. dissertation in December 2009. Jihae has accepted a postdoctoral position with Dr. Joel Richter at the University of Massachusetts Medical Center where she will work on the regulation of RNA processing in the nervous system.